จุฬาลงกรณ์มหาวิทยาลัย

ทุนวิจัย
กองทุนรัชดาภิเษกสมโภช

รายงานผลการวิจัย

การเตรียมและทดสอบคุณภาพของฟิล์มพอลิพิโรล เพื่อใช้ในการตรวจวัดไอระเหยของสารเคมี

โดย

นาย อนุวัฒน์ ศิริวัฒน์
น.ส. ลดาวัลย์ เรืองช่วย

กันยายน 2545

สถาบันวิทยบริการ
จุฬาลงกรณ์มหาวิทยาลัย

ACKNOWLEGEMENTS

This work would not be carried out successfully without the following financial supports: the Rajadapisek Fund of Chulalongkorn University Thailand; a RGJ grant from Thailand Research Fund, no. PHD/4/2541; and a BGJ award, no. BGJ/5/2543.

สถาบันวิทยบริการ
จุฬาลงกรณ์มหาวิทยาลัย

ชื่อโครงการวิจัย	การเตรียมและทดสอบคุณภาพของฟิล์มพอลิพิโรล เพื่อใช้ในการตรวจวัดไอระเหยของสารเคมี
ชื่อผู้วิจัย	นาย อนุวัฒน์ ศิริวัฒน์ และ น.ส. ลดาวัลย์ เรืองช่วย
เดือนและปีที่ทำวิจัยเสร็จ	พฤษภาคม 2544

บทคัดย่อ

พอลิพิโรล ได้ถูกสังเคราะห์ด้วยวิธีทางเคมีและโดปในขั้นตอนเดียวกัน ด้วยตัวโดป 7 ชนิด ในอัตราส่วนโดยโมล ของตัวโดปต่อพิโรล เท่ากัน คือ 1/12 หน้าที่หลักของตัวโดป คือช่วยให้ประจุบวกที่ไนโตรเจนเสถียร นอกจากนี้ ยังพบว่า ตัวโดปยังมีผลต่อคุณสมบัติทางกายภาพ ทางเคมี และทางไฟฟ้าของพอลิพิโรล ตามที่ได้วิเคราะห์ด้วยเครื่องมือหลายชนิดเช่น เครื่องเอ็กซ์เรย์โฟโตอิเล็กตรอนสเปกโตรมิเตอร์ และเครื่องวัดค่าการนำไฟฟ้าจำเพาะแบบสี่ขั้วซึ่งสร้างขึ้นเองในห้องปฏิบัติการ พอลิไพรอลที่โดปด้วยแอลฟา-แนฟทาลีน ซัลโฟเนต และเบทา-แนฟทาลีน ซัลโฟเนต มีคุณสมบัติทางกายภาพ การละลาย ความเสถียรต่อความร้อน ค่าการนำไฟฟ้าจำเพาะ และความเสถียรของค่าการนำไฟฟ้าที่ดี จากการสังเคราะห์พอลิไพรอลที่โดปด้วยแอลฟา-แนฟทาลีน ซัลโฟเนต ในอัตราส่วนโดยโมลของตัวโดปต่อไพรอลต่าง ๆ พบว่า อัตราส่วนโดยโมลของตัวโดปต่อไพรอล ที่ให้ค่าการนำไฟฟ้าจำเพาะ และความเสถียรของค่าการนำไฟฟ้าสูง คือ 1/12 เมื่อให้พอลิไพรอลอยู่ในบรรยากาศของไอระเหยของแอซีโทนในไนโตรเจนที่ความเข้มข้นร้อยละ 16.7 โดยปริมาตร พบว่า ค่าการนำไฟฟ้าจำเพาะลดลง การเปลี่ยนแปลงดังกล่าวขึ้นกับชนิดของตัวโดป อย่างเห็นได้ชัด สำหรับตัวโดปจำพวกซัลโฟเนต ค่าการนำไฟฟ้าจำเพาะที่ลดลง ขึ้นกับ ระดับการโดป (N^+/N) และค่าการนำไฟฟ้าจำเพาะเริ่มต้น ตามความสัมพันธ์แบบเอกซ์โพเนนเทียล และขึ้นกับ สัดส่วนของไบโพลารอน และ ความเป็นระเบียบของโมเลกุล ตามความสัมพันธ์แบบเชิงเส้น และแปรผกผันกับสัดส่วนของส่วนบกพร่อง =N- พอลิไพรอลที่โดปด้วยแอลฟา-แนฟทาลีน ซัลโฟเนต แสดงค่าการนำไฟฟ้าจำเพาะลดลงถึง 0.4 ซีเมนส์ต่อเซนติเมตร เมื่อมีตัวโดปแอลฟา-แนฟทาลีน ซัลโฟเนต มากขึ้นขณะทำการสังเคราะห์ พอลิไพรอลมีปริมาณน้ำในเนื้อสารน้อยลง และแสดงการลดลงของค่าการนำไฟฟ้าจำเพาะได้มากขึ้น จากการศึกษาปฏิกิริยาระหว่างพอลิพิโรล และแอซีโทน ด้วยเครื่องมือหลายชนิด เช่นเครื่องอิเล็กตรอนไมโครสโคปแบบบรรยากาศ พบว่า พันธะไฮโดรเจน การบวมตัว และการสูญเสียประจุบวก เป็นสาเหตุของการลดลงของค่าการนำไฟฟ้าจำเพาะของพอลิไพรอลภายใต้บรรยากาศของแอซีโทน

Project Title	Preparation and Characterization of Polypyrrole Film for Chemical Vapor Sensor Applications
Name of the Investigatiors	Mr. Anuvat Sirivat and Ms. Ladawan Ruangchuay
Year	April 2001

Abstract

Polypyrrole (PPy) was chemically prepared *via* an *in situ* doped polymerization utilizing seven dopant anions (dopant to monomer molar ratio, D/M = 1/12) to stabilize the positive charges on N of pyrrole rings. These dopant anions were found to play important roles on physical, chemical, and electrical properties of PPy as revealed by several techniques, e.g. X-ray photoelectron spectrometer and the custom-made four-point probe conductivity meter. PPys doped with α-naphthalene sulfonate (PPy/A) and β-naphthalene sulfonate (PPy/B) have good pellet appearance, solubility, thermal stability, specific conductivity, and stability in conductivity. PPy/A was chemically synthesized at various D/M ratios. The D/M ratio giving PPy/A with high specific conductivity and stability in conductivity is 1/12. Upon exposure to acetone vapor at 16.7 vol.% in N_2, negative changes in specific conductivity, $\Delta\sigma$, of PPys were observed. These changes depend critically on the type of the dopants used. For the sulfonate dopants, $\Delta\sigma$ exponentially depended on the doping level (N^+/N) and the initial specific conductivity. It depended linearly on the proportion of the bipolaron species and the ordering and inversely on the proportion of the imine-like nitrogen defect (=N-). PPy/A exhibited the largest specific conductivity decrement: 0.4 S/cm. With a higher D/M ratio, PPy/A contained a smaller amount of moisture content and its response to acetone was enhanced. Various techniques, e.g. an environmental scanning electronmicroscope, were used to investigate the interaction between PPy and acetone molecules. H-bonding, Swelling, and reduction reaction by acetone are suggested to cause the decrease in specific conductivity of PPy.

TABLE OF CONTENTS

LIST OF TABLES

สถาบันวิทยบริการ
จุฬาลงกรณ์มหาวิทยาลัย

LIST OF FIGURES

FIGURE PAGE

FIGURE PAGE

สถาบันวิทยบริการ
จุฬาลงกรณ์มหาวิทยาลัย

LIST OF SYMBOLS

σ	Specific conductivity (S/cm)
$\chi_{corr,M}$	Corrected molar magnetic susceptibility (cgs $mole^{-1}$)
λ	Wavelength (nm)
θ	Contact angle (degree)

สถาบันวิทยบริการ
จุฬาลงกรณ์มหาวิทยาลัย

CHAPTER I
INTRODUCTION

Presently, safety requirements of human being become more and more stringent. There are many circumstances in which a gas sensor* is desired for detecting a specific gas or gases in an environment; for instance, various pollutants in the atmosphere, the leakage of anesthetic gases in hospital, the leakage of toxic gases in laboratory, and the emission of odors from food indicating its condition. Many combustible and toxic gas detectors using metals and polymers have been developed. Some of these have been described (Loughlin, 1993).

The most widely used gas monitor is an *electrochemical sensor* with an anode and a cathode separated by an electrolyte. The current generated by this system depends on the concentration of gas absorbed and oxidized or reduced on the electrode surface. If the oxygen level is less than 1%, it will need a fresh air purging for 30 minutes every hour. A *metal oxide semiconductor* (e.g. tin oxide and zinc oxide) is a popular gas detector. Its electrical conductivity changes when gas molecules are adsorbed onto its surface. Even though its low selectivity has been improved (Pijolat *et al.*, 1999), its operating temperature needs to be as high as 300 – 400 °C which remains a problem. Moreover, it usually takes a few days to obtain a really stable readout signal. A *catalytic detector* works on the basic of oxidation reaction of flammable gas which releases energy and raises its temperature. However, the early catalytic sensors could be poisoned temporarily by compounds containing halogen or sulfur. The example of this class is a catalytic pellistor sensor (http://www.crowcon.com) which has to be operated at 500 °C.

Spanning more than two decades, *conductive polymers* have been developed with the aim to be an intelligent gas sensor because of many advantages: they can be operated at room temperature; they are light, non-corrosive and can be prepared and cast on various substrates easily. Polypyrrole, PPy, has been one of the most interested amongst several conductive polymers due to its high electrical conductivity (Truong *et al.*, 1992), relatively high environmental stability (Truong *et al.*, 1995), and the ease of being doped under various dopants.

---

* In this specification, the term "gas" refers to material which is in the gas state at room temperature, including vapor and odor.

1.1 Theoretical Background

1.1.1 Electrically Conductive Polymers

Electrically conductive polymers are polymers that possess electrical conductivity due to the fact that there are π-electrons delocalizing along the backbone. They are the conjugated polymers which can be chemically or electrochemically synthesized. The neutral forms of conductive polymers can be insulator or semi-conductor. The examples of this class of polymer are polyacetylene, polythiophene, PPy, and polyaniline. The chemical structures of their neutral forms are shown in Figure 1.

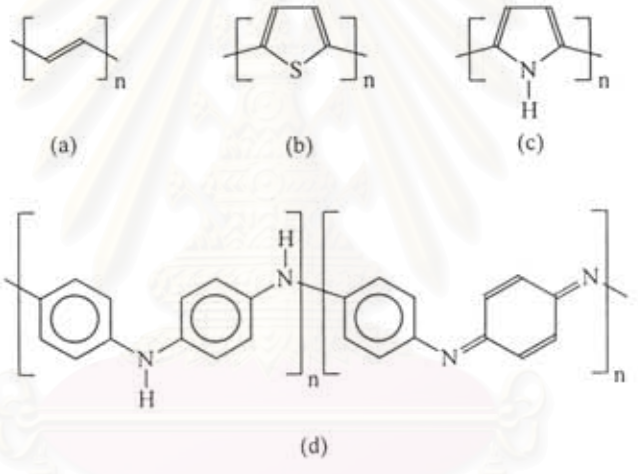

Figure 1 The chemical structures of the neutral form of: a) polyacetylene; b) polythiophene; c) PPy; and d) polyaniline.

Delocalized charge carriers could be introduced by donating electrons to or withdrawing electrons from polymer chain via reduction or oxidation reaction, respectively. This process is known as 'doping process'. When electrons are removed from the valence band by an oxidizing agent, p-type conducting polymer is formed with positive charges which can delocalize as charge carriers. *Vise versa* when electrons are added by a reducing agent, n-type conducting polymer is formed. For most of conductive polymers, the former structure is more thermodynamically stable and it is much more widely studied. Oxidation breaks one double bond in polymer chain, leaving a free radical and a positive charge on the chain. This form is called

'polaron'. At a higher extent of oxidation, when a concentration of polaron is so high that they can meet with each other, two of radicals in particular two polarons combine with each other to form one covalent bond. This form of charge carries consists of two positive charges remaining from the combination of those two polarons: it is called 'bipolaron'. These induced charge carriers must be stabiiized by ions from the reaction medium. These counter ions are called 'dopant'. The large range of conductivity is obtained by a doping process, which mainly depends on type of dopant (Yamaura *et al.*, 1988; Wang, *et al.*, 1990; Cao *et al.*, 1992; Shirakawa *et al.*, 1994) and dopant concentration used (Heeger and MacDiarmid, 1980). Polyacetylene can have the specific conductivity as high as 10^4 S/cm when it is doped with I_3^- (Shirakawa *et al.*, 1994). The highest specific conductivity of PPy that has been reported is 10^3 S/cm when it is doped with PF_6^- (Yamaura *et al.*, 1988).

1.1.2 Polypyrrole

Polypyrrole, PPy is one of poly(heterocycles) that possess high environmental stability over polyacetylene which composes of only hydrocarbon. PPy can be easily synthesized via electrochemical (Dall'Olio *et al.*, 1969; Diaz *et al.*, 1979) or chemical oxidative coupling polymerization (Angeli, 1916). These advantages make it, nowadays, the most frequently used in commercial applications (Rodríquez *et al.*, 1997).

The principal advantage of a chemical synthesis over an electrochemical one is the possibility of mass production at low cost. The neutral form of PPy obtained from chemical oxidative coupling polymerization has the specific conductivity on the order of $10^{-10} - 10^{-11}$ S/cm. The general scheme of polymerization mechanism is shown in Figure 2. Upon an oxidative doping, a more stable p-type doped form of PPy is formed with polaron or bipolaron as charge carriers. The structure of PPy along with the charge carriers and all possible chemical defects, e.g. branching, carbonyl group, are shown in Figure 3.

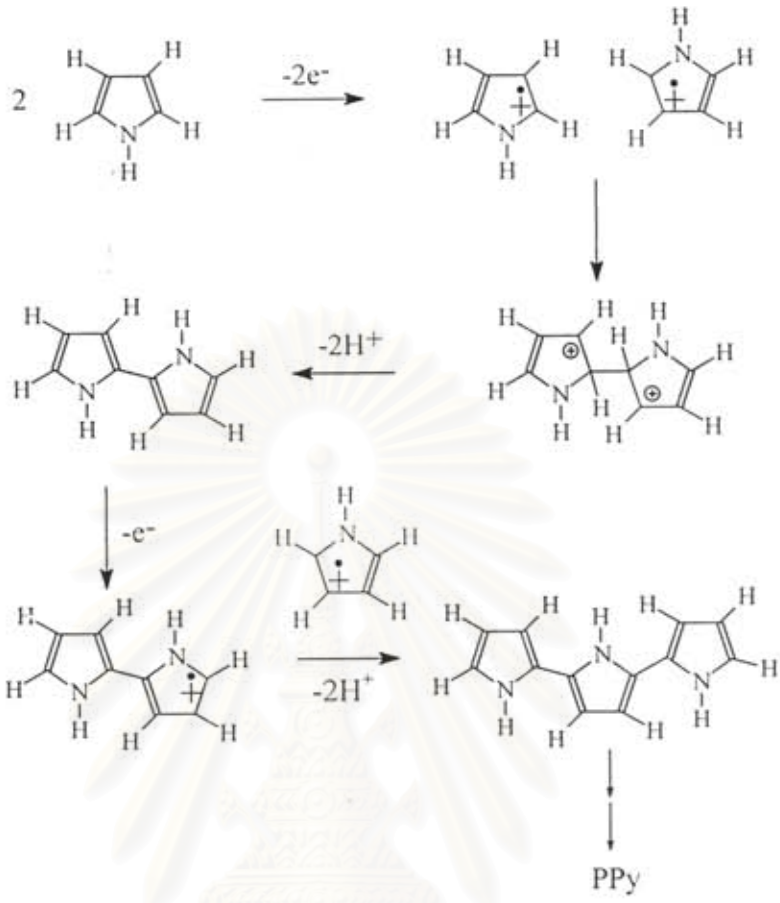

Figure 2 The proposed mechanism of chemical oxidative coupling polymerization of PPy (Zotti, 1997).

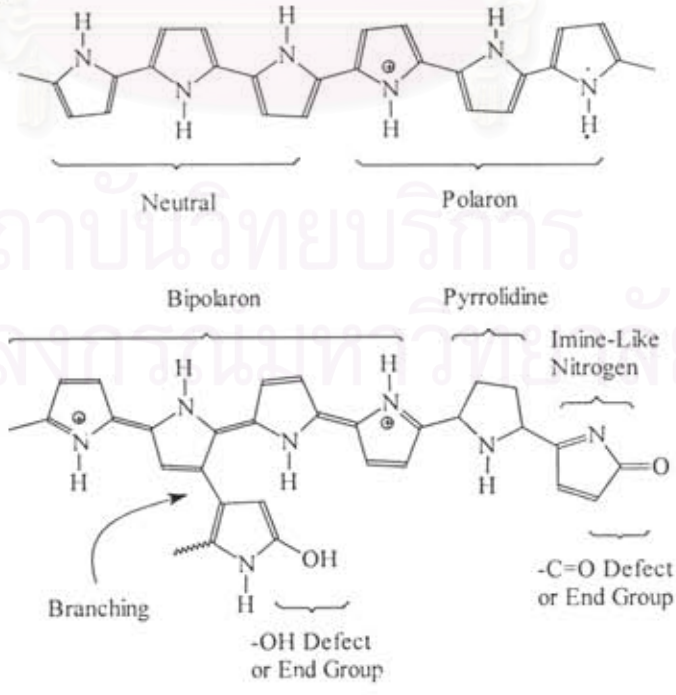

Figure 3 The structure of PPy with its possible chemical defects.

1.1.3 Application of Conductive Polymers as Gas Sensor

The electrical conductivity sensitivity of conductive polymers when they are exposed to various chemicals has been a subject of many studies which focus on sensing applications (Kanazawa *et al.* 1979/1980; Miasik *et al.*, 1986; Gustafsson and Lundström, 1987; Hanawa *et al.*. 1988; Philip *et al.*, 1989; Hanawa and Yoneyama, 1989). There are three mechanisms for the specific electrical conductivity to change when a conductive polymer is exposed to a gas. The first mechanism occurs with gas molecules with specific charge transfer properties. Electron-accepting gases like NO_2 (Hanawa *et al.*, 1988) withdraw electrons from polymer chains. If the conductive polymer is a p-type-doped polymer which have positive charges as the charge carriers, its electrical conductivity will increase with NO_2. The FT-IR spectral investigation evidently shows that NO_2 oxidatively dopes the conductive polymer and becomes the dopant anion NO_2^- (Miasik *et al.*, 1986; Hanawa *et al.*, 1988). On the other hand, electron-donating gases like ammonia (NH_3) (Hanawa and Yoneyama, 1989) reduce the amount of positive charges in p-type-doped polymer chains and hence decrease the electrical conductivity.

The second mechanism possibly involves conformation changes and/or degree of crystallinity in the polymer matrix itself due to the incorporation of guest molecules which do not have the distinct charge transfer properties by themselves. This mechanism induces a greater or lower charge mobility which in turn enhances or reduces electrical conductivity.

The third mechanism involves the migration of dopant anion molecules which are attached electrostatically to a polymer chain; this process can be referred as an ionic conductivity (Cassignol *et al.*, 1998).

1.1.4 Flammable Chemicals

One of the main causes of fire accident on construction sites and also in chemical stores is the presence of the flammable chemicals, e.g. acetone. Acetone and toluene are the main ingredients in lacquer, the material used for interior decoration. When their concentrations in the air are between their lower and upper explosive limits: 2.5 - 12.8 vol.% for acetone and 1.1 - 7.6 vol.% for toluene (Chou 2000), they can be instantly ignited. Within this decade, there have been at least two

serious fire accidents during hotel constructions in Bangkok, Thailand. There have been a number of fire accidents in chemical stores all over the country.

1.2 Literature Survey

1.2.1 Preparation of PPy

The first report on the chemical oxidation of pyrrole appeared in 1888, then the subsequently reports on the polymerization in the presence of hydrogen peroxide to yield what was commonly referred to as 'pyrrole black' had to wait until 1916. More than 50 years later, the first report of electrochemical production of PPy appeared (Dall'Olio *et al.*, 1969). Until now, many other ways to synthesize PPy have been developed. Sun and Ruckenstein (1996) polymerized PPy films on a surface of a hot 2 wt.% poly(vinyl alcohol). However the highest electrical conductivity from this method was only 1 S/cm. More recently, the *in-situ* doped polymerization has been suggested by Shen and Wan (1997). Dopant was introduced into PPy matrix during polymerization. This method provides the β-naphthalene sulfonate doped PPy with the specific conductivity as high as 27 S/cm.

1.2.2 Application of PPy as Gas Sensor

During the 1970s, reports began to appear on the gas detecting properties of PPy. Miasik *et. al.* (1986) investigated interactions between ammonia, nitrogendioxide (NO_2) and hydrogensulphide (H_2S) and PPy coated onto electrodes, and the responses were found to be reversible. However the electrical conductivity response to NH_3 concentration was nonlinear. Later, many studies have focused on mechanisms of these interactions, especially that caused by NH_3 (Gustafsson and Lundström,1987; Hanawa and Yoneyama, 1989). In 1987, Josowiez *et. al.* demonstrated that under suitable electropolymerization conditions, where aromatic solvents such as nitrotoluenes were incorporated into the PPy metric, PPy exhibited the selective sensitivity to vapor of aromatic compounds. The responses of PPy films to 4 kinds of organic vapors were studied by Philip and Sim in 1989. Methanol and ethanol vapors gave a stable and reproducible decrease in film conductivity but the response of ethanol was much slower. For toluene, acetone and ether vapors, the

responses were much smaller. Moreover for acetone, the baseline resistance of the film drifted towards lower conductivity. In the recent years, Slater and Watt (1992) studied the response of bromine doped PPy, which was coated on piezoelectric quartz crystal microbalance on methanol, hexane, 2,2-dimethylbuthane, ammonia and hydrogensulfide. There were changes in both conductivity and mass. The reduction in specific conductivity of PPy caused by NH_3 was nearly reversible (Gustafsson and Lundström, 1987). However, irreversible changes may result with a prolonged exposure time, concentration of NH_3, and the presence of water vapor (Gustafsson and Lundström, 1987). Other gases studied were AsF_5, Br_2 (Kanazawa, *et al.*, 1979/1980), O_2 in N_2 (Blanc *et al.*, 1990), CH_2Cl_2, and HCN (Langmaier and Janata, 1991).

The studies of the guest vapor molecules having no distinct charge transfer properties are: cyclohexane and ethyl acetate (Blanc *et al.*, 1990); haxane, triethylamine, butanal, butan-1-ol, hexan-1-ol, and nonan-1-ol (Deng *et al.*, 1997); ethyl acetate, acetone, and ethanol (Musio and Ferrara, 1997); and water (Okuzaki *et al.*, 1997; Okuzaki *et al.*, 1999). Nigorikawa *et al.* (1995) found an increase in resistivity of PPy upon an acetone vapor exposure. A lower electronegativity of acetone as compared to the work function of PPy suggests the reduction of PPy caused by acetone. An exposure of Langmuir-Blodgett film of PPy to acetone (Milella *et at.*, 1996) caused a stable and reproducible resistance changes. The response increased with chemical's polarity; for acetone, the response was smaller than for those of methanol and ethanol, but bigger than those of ethyl acetate and toluene. The good correlation between resistance changes and the number of monolayers in the film indicated a bulk effect.

สถาบันวิทยบริการ
จุฬาลงกรณ์มหาวิทยาลัย

1.3 Research Philosophy

1.3.1 The Driving Force of Research Work

Because of the grave dangers from fire accidents described above, a sensor for those flammable chemicals is needed. An appropriate sensor should be simple, cheap, light and portable, so that every construction sites and chemical stores in poor countries can afford to use it practically.

1.3.2 Objectives

Our objectives for this work are: to develop high sensitive PPy-based sensors for detecting acetone vapor, which is flammable chemical in lacquer; and to investigate the reaction between acetone and PPy.

1.3.3 Research Strategies

It has been shown that different chemical structures and properties of dopants can modify the properties of PPy, e.g. the surface morphology (Topart and Josowicz, 1992), the solubility (Shen and Wan, 1998), the moisture content (Cassignol *et al.*, 1998), and the degree of water sorption (Okuzaki *et al.*, 1999). However, the properties of PPy doped with various dopants from various research groups cannot be compared directly due to some differences in polymerization conditions, handling, processing and storage conditions. This work aims to report the effect of dopant anions and dopant concentrations on the physical, chemical, and electrical properties of PPy. Then, the PPy with acceptable properties will be selected to further study its electrical response of PPy toward acetone vapor.

To accomplish the latter objective, various techniques, e.g. an environmental scanning electronmicroscope, a thermogravimetric analyzer, a Fourier transform infrared spectrometer, an X-ray diffractometer, were used to investigate the interaction between PPy and acetone molecules.

CHAPTER II
PROCEDURE

Part I Synthesis and Characterization of Polypyrrole

2.1.1 Materials

Pyrrole monomer (AR grade, Fluka) was purified by distillation under the reduced pressure prior to use. Ammonium persulfate, APS (AR grade, Aldrich) was used as the oxidant and *m*-cresol (AR grade, Fluka) was used as the solvent in the film casting; they were commercially available and used without further purification. The dopants used were α-naphthalene sulfonic acid, sodium salt (AR grade, Fluka), β-naphthalene sulfonic acid, sodium salt (AR grade, Fluka), camphor sulfonic acid (AR grade, Fluka), dodecylbenzene sulfonic acid, sodium salt (AR grade, Fluka), ethane sulfonic acid (AR grade, Fluka), perchloric acid (AR grade, Fluka), and *p*-aminobenzoic acid (AR grade, Fluka). These chemicals were used as received.

2.1.2 The Polymerization Procedure

The doped PPy with various dopant anions were chemically synthesized by the *in situ* doped, oxidative coupling polymerization according to the method of Shen *et al.* (1997). The solution of 0.6846 g (3.0 millimole) ammonium persulfate in 10.0 ml deionized water was slowly added to the mixture of 1.2 millimole of dopant anion and 1.0 ml (14.5 millimole) pyrrole in 20.0 ml deionized water. The reaction was carefully maintained at 0 °C (±0.5 °C) for 2 hours. The contact time between the growing polymer and the oxidant was shortened from the reference method to minimize a possible degradation of PPy. The obtained PPy was precipitated by pouring the reaction mixture into a large excess amount of deionized water. The PPy powder was washed several times with deionized water and methanol before drying in a vacuum at room temperature for 2 days. The undoped PPy was synthesized by the same procedure but in the absence of a dopant anion. The dedoped PPy was prepared by

treating undoped PPy with 2 M NH_4OH for 12 hours. The notations used for all PPys are tabulated in Table 1. In order to study effect of molar ratios of dopant anion to pyrrole monomer (D/M ratios) on the properties of PPy, PPy was synthesized with various amounts of α-naphthalene sulfonic acid, sodium salt. The D/M ratios were chosen to be 1:96, 1:48, 1:24, 1:12, 1:6, 1:3, 1:2, 2:3, and 1:1.

2.1.3 The Characterizations of PPys

2.1.3.1 Physical Properties

The morphologies of the PPy pellets were studied by using the scanning electron microscope (SEM, JOEL model JOEL 520). The accelerating voltage and the magnification used were 20 kV and 3500 times, respectively. A thermogravimetric analyzer (TGA, Perkin-Elmer model TGA7) was used to determine the moisture content and the onset temperature of PPy degradation. The furnace temperature was varied between 25 to 700 °C with a heating rate of 10 °C/min under the N_2 atmosphere. The moisture content was determined from the weight loss of PPy when temperature was increased from 25 to 150 °C. A X-ray diffractometer (XRD, Rigaku model D/MAX-2000) was used to characterize the ordering in amorphous PPy. Samples, in the forms of pellet pressed at 60 kN, having a diameter of 1.3 cm and thickness of ~0.5 mm, were mounted onto metal sample holders. The X-ray source was Cu K-Alpha 1. The diffraction pattern was taken in the 2θ range of 5 – 40 degrees with the scanning speed of 5 degree/min.

2.1.3.2 Chemical Properties

The functional groups of synthesized PPy were characterized by a Fourier transform infrared spectrometer (FT-IR, Bruker model FRA 106/S). The FT-IR absorption was taken for 20 scans at the wavenumbers between 400-4000 cm^{-1} with the resolution of 4 cm^{-1}. A ultraviolet-visible spectrometer (UV-Vis, Perkins-Elmer model Lambda 16) provided the characterization of charge carrier species. Transparent films of PPys were prepared by means of the solution casting. 1 mg of PPy was dissolved in 20 ml of *m*-cresol. To obtain a completely clear solution, the solution was filtered through a PTFE membrane with the pore size of 1.0 μm. After

smearing this solution onto a glass slide, the solvent was allowed to evaporate in a vacuum oven at 60 °C for 5 hours. Each visible spectrum was taken in the range of 350 – 900 nm with a scan speed of 1440 nm/min. Another instrument used for the investigation of charge carrier species was a magnetic susceptibility balance (MSB, Johnson Matthey Chemicals). The positive value of the corrected molar magnetic susceptibility, $\chi_{corr,M}$ reveals the paramagnetic property of materials (Jolly, 1970), e.g. the material containing polaron species. On the other hand, the negative value indicates a diamagnetic property, but it cannot be used to distinguish the bipolaron state from the neutral state. The doping level can be determined by an elemental analyzer (EA, Perkins-Elmer model PE 2400 series II CHNS/O) and the scanning electron microscope (EDS/SEM, JOEL model JOEL 520) in the energy dispersive mode. For PPy doped with sulfur-containing dopant, the apparent doping level is defined as the number of S atoms per 1 atom of N, *S/N*. For PPy doped with perchlorate and PPy doped with *p*-aminobenzoate, it can also be defined as *(S+Cl)/N x 100* and as *[S+1/2 O]/[(N-1/2 O)] x 100%*, respectively. Note that the number of S atoms in PPy doped with a non sulfur-containing dopant is also taken into account because there is the presence of HSO_4^- and SO_4^{2-} acting as the co-dopants (Ayad, 1994, Prissanaroon *et al.*,2000). The most powerful instrument for the determination of chemical compositions, doping levels, and charge carrier species is the X-ray photoelectron spectrometer (XPS, Perkin Elmer model PHI 5400). The non-monochromatic MgKα with photon energy of 1253.6 eV was selected as the X-ray source. The X-ray source power was 300 W (15 kV x 20 mA). The pass energy used was 17.90 eV. The take-off angle was 45°. The sensitivity factor values for the Omni-Focus Lens A are 0.477 for N 1s and 0.570 for S 2p spectra.

2.1.3.3 Electrical Properties

In order to study the electrical properties of PPy, 0.05 g of PPy powder was ground and pressed by a hydraulic press at 60 kN into a pellet with the diameter of 2.5 cm and a thickness between 60 – 90 μm. The thickness of each pellet was measured by a thickness gauge (Peacock model PDN 12N) having a resolution of 0.001 mm. The specific conductivity, σ of the PPy pellet was measured by a custom-made four-point probe conductivity meter (Prissanaroon *et al.*, 2000). Si and SiO_2

sheets with known resistance values were used in the probe calibration. The current, which was applied to the outer terminals of the probe, and the voltage drop between the inner terminals of the probe were detected The suitable current used was determined for each PPy; it was set at a level so that each PPy still had its Ohmic behavior without the Joule heating effect. For instance, the current used for PPy/U and PPy/A was 2 (± 0.5) mA and 20 (± 1) mA, respectively. The specific conductivity values were measured at the age of about two months after they have virtually ceased to change, and at the age of more than one year to see roughly the electrical stability of each PPys after a long-term storage in the ambient pressure, temperature, and humidity.

สถาบันวิทยบริการ
จุฬาลงกรณ์มหาวิทยาลัย

Part II Electrical Response of Polypyrrole to Acetone Vapor

2.2.1 Effect of Dopant Anions and Dopant Concentrations on the Response of PPys toward Acetone Vapor

PPy powder was ground and pressed by a hydraulic press at 60 kN to be a pellet with a diameter of 2.5 cm. An aging period greater than 50 days of PPys was allowed so that the specific conductivity of PPy attained its steady value, prior to the study of electrical response to acetone vapor.

The flow system, as shown in Figure 2.1, consists of a humidity-control set (A-C), an acetone container (D), and an exposure chamber (F) which contains the four-point probe (linear array) and the thermohygrometer inside. 4.00 ml of acetone in the container was slowly vaporized and flowed into a closed loop system having a total volume of 7728 cm^3. The acetone concentration in N_2 was 17 vol.%. The controlled temperature and humidity were 25 °C (± 1 °C) and 50 %RH (± 10 %RH), respectively. The change in the specific conductivity was monitored by a data acquisition system (Data Translation board model DT2801) interfaced with a personal computer and reported in terms of $-\Delta\sigma$.

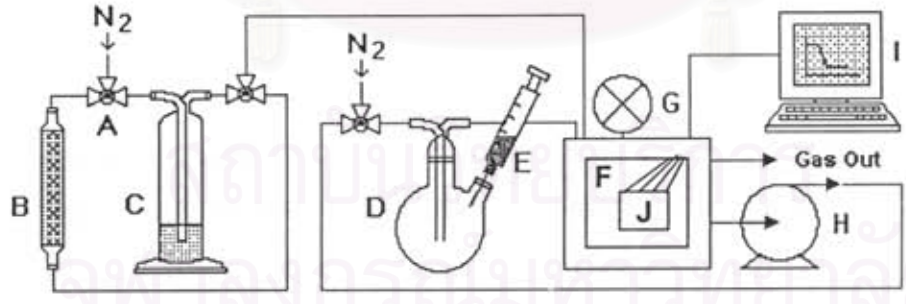

Figure 2.1 The schematic draw of the flow system: A) the three way value; B) the dryer column; C) the water reservoir; D) the 2-neck round bottom flask; E) the syringe for acetone injection; F) the exposure chamber consisting of the thermohygrometer; G) the pressure gauge; H) the diaphragm pump; I) the data acquisition system; and J) the four-point probe conductivity meter with PPy pellet.

2.2.2 Effect of Acetone Vapor Concentrations on the Response of PPys

Only undoped and some doped PPys were selected for this experiment. The volume of acetone vapor in the container was varied in order to vary the acetone vapor concentration in the system from 10% of LEL (0.25 vol.%) to the saturated concentration of acetone vapor at 25 °C (30 vol.%). The controlled temperature and relative humidity for this system were 25 °C (± 1 °C) and 50 %RH (± 10 %RH), respectively. The parameters obtained from this experiment were the response pattern (linear/non-linear), the sensitivity (the slope of the plot between $\Delta\sigma$ and acetone vapor concentration) and the maximum detectable concentration. The first two parameters are assigned only in the concentration range of LEL – UEL of acetone vapor.

2.2.3 Interaction between Acetone Vapor and PPy

The conditions for each experiment were designed to suit the performance and signal stability of each instrument. The change in morphology after the prolonged exposure to acetone of PPy pellet pressed at 30 kN/1.3 cm^2 was studied by ESEM. The water vapor pressure used was 400 – 800 Pascal. The pictures of pellet surface were taken before and after exposing to the saturated acetone vapor in N_2 for 24 hours at the magnification of 46x and 3500x. For the XPS experiment, the change in the proportions of chemical species: neutral nitrogen, polaron species, bipolaron species, and imine-like nitrogen (=N-) were monitored from the PPy sample treated under the same conditions as those in the ESEM experiment. To study the type of absorption of acetone onto PPy (physisorption or chemisorption) and bonding, the TGA thermograms and the FT-IR spectra of PPy powder before and after exposing to the saturated acetone vapor in N_2 for 24 hours were recorded. The XRD experiment was performed on the PPy/A pellet before and after immersing in acetone liquid for 30 minutes, in order to study the change in the microstructure of PPy. The changes in visible spectra of PPy/B film, cast from *m*-cresol solution on a glass slide, were monitored during an exposure to the saturate acetone vapor.

CHAPTER III
RESULTS AND DISCUSSION

Part I Characterization of Polypyrrole

1.1 Effect of Dopant Anion on Properties of PPy

1.1.1 Physical Properties

1.1.1.1 Appearance, Morphology, and Pellet Density

All of PPys, including PPy/U and PPy/De, are black. Notations of various PPys synthesized and doped are listed in Table 1. PPy/A and PPy/B are relatively softer than the others. After they were pressed into pellets, PPy/A and PPy/B pellets turned out to be very shiny and slightly bendable. The pellets of other PPys, especially PPy/U and PPy/De, are on the other hand dull and very brittle. PPy/D pellet is shiny but very brittle. The physical, chemical and thermal properties investigated are summarized in Table 1. As revealed by SEM, the surface morphologies of all PPy powder are globular (see those of PPy/U and PPy/B in Figures 1a and 1c as examples). The sizes of globules of PPy/A and PPy/B (Figure 3.1c) are smallest whereas that of PPy/D (Figure 3.1e) is largest. The surface morphologies of the pellets of PPy/U, PPy/A and PPy/D, are shown in Figures 1b, 1d and 1f, respectively. Their morphologies are similar to those of powder form but appear smoother and denser. The pellet densities, as calculated from the pellet weights and pellet thickness values, are tabulated in Table 1. The density of pellet is lowest for PPy/De and highest for PPy/A, PPy/B, and PPy/AB pellets.

There are correlations between the pellets' appearances, morphologies, and densities. When PPys contain irregular globules, their pellets have lower density, dull and brittle. On the other hand, when PPys contain regular and soft globules, their pellets have higher pellet density, shiny and bendable. The examples of the former case are PPy/De and PPy/U, whereas those of the latter case are PPy/A and PPy/B. The smooth surface of PPy/D pellet shows that the observed big globules of PPy/De in Figure 3.1e are the crushable aggregates of the very fine PPy particles. Dodecylbenzene sulfonate is an effective surfactant; it provided an effective

emulsion polymerization of pyrrole monomer in water. The droplets of pyrrole monomer in water were smaller than those in the polymerization with other dopants, resulting in fine PPy particles. Due to its ultra-fine particle size, PPy/D needed ca. 3 times longer time for filtration with the 0.2 μm membrane. PPy/D pellet also has high density; it is shiny but very brittle due to the failure of particle continuity (see Figure 3.1f).

สถาบันวิทยบริการ
จุฬาลงกรณ์มหาวิทยาลัย

Table 1 The notations for the dedoped PPy, the undoped PPy, and the doped PPys with various dopants, along with the moisture content and the onset temperature of degradation of dopants, and the physical properties of PPys: the pellet appearance, the solubility in m-cresol, the moisture content, the onset temperature of degradation ($T_{degrade}$) when D/M ratio was 1/12

Notation of material	Dopant			Pellet appearance	Pellet density (g/cm^3)	Solubility in *m*-cresol	Moisture content (wt %)	$T_{degrade}$ (°C)	Disordering proportion from XRD
	Name	Moisture content (wt%)	$T_{degrade}$(°C)						
PPy/De	(dedoped PPy)	N/A	N/A	very dull and brittle	0.86	Insoluble	10.1	175.1	0.45
PPy/U	(undoped PPy)	N/A	N/A	dull and brittle	0.93 *(0.02)*	Insoluble	4.9 *(0.4)*	222.3 *(7.9)*	0.31 *(0.02)*
PPy/A	□-naphthalene sulfonate	3.2	459.0	very shiny and bendable	1.28	Soluble	3.9 *(0.1)*	249.5 *(0.7)*	0.22 *(0.01)*
PPy/B	□-naphthalene sulfonate	0.3	526.4	very shiny and bendable	1.24 *(0.04)*	Soluble	3.0 *(0.4)*	260.2 *(16.2)*	0.23
PPy/C	camphor sulfonate	4.1	196.3	dull and brittle	1.09	Insoluble	4.8 *(1.2)*	202.9 *(5.0)*	0.26 *(0.03)*
PPy/D	dodecylbenzene sulfonate	3.2	415.0	shiny but very brittle	1.15 *(0.08)*	Soluble	0.9 *(0.1)*	270.9 *(7.1)*	0.24 *(0.03)*
PPy/E	ethane sulfonate	N/A	N/A	dull and brittle	1.03 *(0.03)*	Insoluble	5.6 *(0.7)*	214.8 *(7.6)*	0.24 *(0.02)*
PPy/P	perchlorate	N/A	N/A	dull and brittle	1.11	Insoluble	5.4 *(0.0)*	231.8 *(2.5)*	0.22
PPy/AB	*p*-aminobenzoate	0.7	171.0	shiny but brittle	1.26 *(0.07)*	Insoluble	4.6 *(1.0)*	213.7 *(2.8)*	0.24

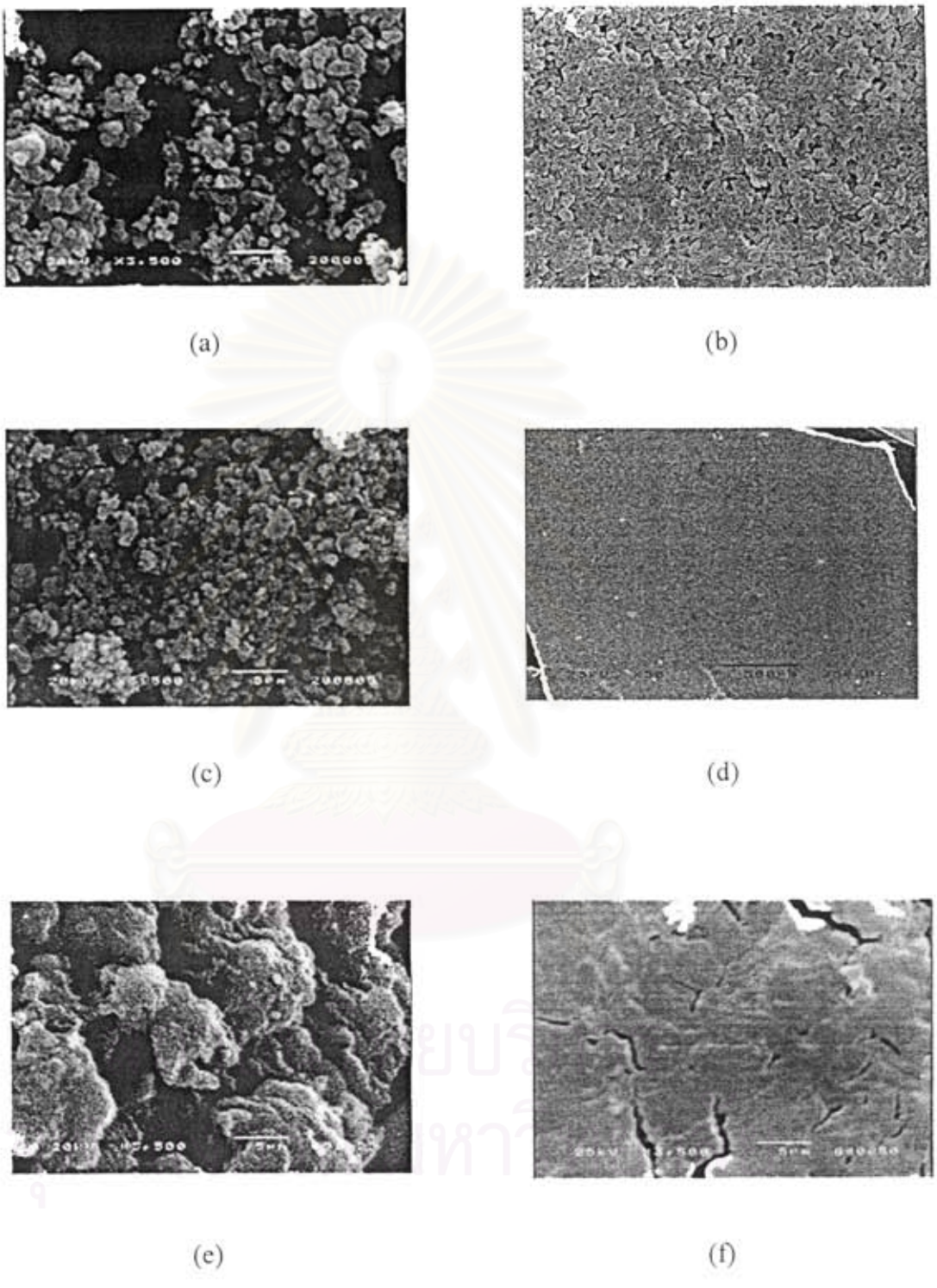

Figure 3.1 The scanning electron micrographs of: a) PPy/U powder (3500x); b) PPy/U pellet (3500x); c) PPy/B powder (3500x); d) PPy/A pellet (50x); e) PPy/D powder (3500x); and f) PPy/D pellet (3500x).

1.1.1.2 Solubility

Most of PPys reported in many previous works (Shen and Wan, 1997; Shen and Wan, 1998) are insoluble in most common solvents. This is believed to be caused by an intense interchain cohesion, high anisotropy of interchain interactions, and/or crosslinking (Qian, 1993). In *m*-cresol, the good solvent for PPy (Shen and Wan, 1997; Shen and Wan, 1998), there are only three PPys in this work that are soluble, i.e. PPy/A, PPy/B, and, especially, PPy/D (see Table 1). These three PPys consist of the big aromatic sulfonate dopants (and long alkyl chain for PPy/D) which destroy the interchain interaction between PPy chains and hence increase the solubility of PPy as suggested by Shen and Wan (1998).

1.1.1.3 Moisture Content

Moisture content values of all PPys are shown in Table 1. The PPy/U, PPy/C, PPy/E, PPy/P, and PPy/AB have approximately the same moisture contents; 4.6-5.6 wt % while the PPy/A, PPy/B, and PPy/D have significantly lower moisture contents; less than 4 wt % whereas PPy/De has the highest moisture content; ca. 10 wt %.

The N-H group in PPy may possibly have the H-bonding interaction with water. The bound water cannot be completely removed at the room temperature (Cassignol *et al.*, 1998). The amount of this bound water in term of moisture content can be affected by the dopant type (Cassignol *et al.*, 1998). The lowest moisture content, which was found in PPy/D, is possibly caused by the long hydrophobic chain of dodecylbenzene sulfonate dopant. Other PPys doped with short chain organic dopants or inorganic dopants have slightly higher moisture contents. The significantly high moisture content in PPy/De could be the result of the additional base treatment in the dedoping process, which was carried out in water. It was noticed that its pellet density is very low; however, there is no clear correlation between moisture content and pellet density.

1.1.1.4 Thermal Stability

Degradation temperatures of all PPys are tabulated in Table 1 along with those of some solid dopants. Comparing with PPy/De, all doped PPys and PPy/U have higher degradation temperatures, especially, PPy/A, PPy/B and PPy/D: they have $T_{degrade}$ higher than 250 °C. These three PPys were doped with the aromatic sulfonate dopants which have the onset of degradation temperature more than 300 °C.

1.1.1.5 Order Aggregation

The X-ray diffractograms of PPy/U and PPy/A as the representative of doped PPys are shown in Figures 2a and 2b, respectively, with their deconvoluted results underneath. All of the PPys exhibit similar X-ray diffractogram; however, there are some differences when examined in detail.

The broad maximum at $2\theta = 25.4 - 27.8^{\circ}$ corresponds to the d-spacing of 3.2 – 3.5 Å, which is close to the van der Waals distance of the aromatic groups (Gassner *et al.*, 1997). For all PPys, it can be referred to the distance between the aromatic pyrrole rings in different segments (an interplanar spacing). The breadth of peak has an anti-correlation to the extent of crystal by Scherrer equation (Campbell and White, 1991). The crystal extent was measured in the direction perpendicular to the plane corresponding to the diffraction peak: it was found to vary between 12 – 15 Å for these PPys. Due to its extremely small crystal size, it is considered as the disorder segment in PPy matrices. The proportions of the disorder peak in PPys are shown in Table 1 as the disorder proportion. PPy/De has the highest disorder proportion whereas PPy/A and PPy/B have the highest order proportions. The proportions of disorder segment polynomially correlate with the pellet density (fit goodness or $R^2 = 0.91$) and the moisture content values ($R^2 = 0.85$). For instance, PPy/D has the largest disorder area; it also has the lowest pellet density and the highest water susceptibility. However, it should be noted again that there is no correlation between the pellet density and the moisture content by any types of regression ($R^2 < 0.65$).

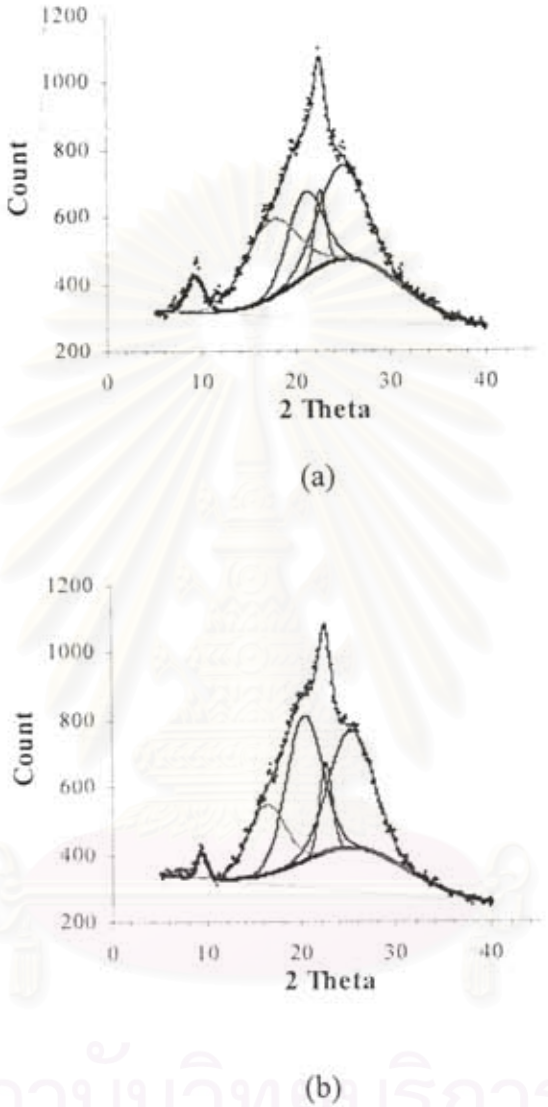

Figure 3.2 The X-ray diffractograms of: a) PPy/U pellet; and b) PPy/A pellet, along with their deconvoluted results underneath.

The next broad maxima is located at the same 2θ as the first one but it is sharper and has a more well defined d-spacing (3.5 Å) and its crystal extent is 2 –3 times larger. For the pellets of PPy/A, PPy/B, and PPy/C, the crystal extents are 30 – 34 Å. They are 22 – 28 Å for the others.

The peak locating around 2θ of 22.5 – 22.7° is a very sharp one. It corresponds to d-spacing of 3.9 Å and the crystal size of as high as 99 –125 Å, with no correlation to the dopant sizes. The interpretation for this peak is unclear. It could be the distance between neighboring pyrrole rings in the conjugating system of PPy, where the α-α' linkages are double bonds. Nevertheless, its intensity proportion is very small: 2.1 % for PPy/De, 7.2 % for PPy/D, and 4.9 - 6.5 % for the others. The percentages of these peaks exponentially correlate with the degradation temperatures (R^2 =0.70). This reveals that these double bond linkages built up the hard segments in PPy which induced high thermal stability to PPy.

The next line-broadening at 2θ of 20.0 – 21.0° (d-spacing = 4.2 – 4.4 Å) can be identified as the Miller index of 110 for a hexagonal structure (Davidson *et al.*, 1996) and the distance between neighboring pyrrole rings on the same chain (Gassner *et al.*, 1997) when α-α' linkages are single bonds and flexible. As calculated from its width (Campbell and White, 1991), this type of order consists of 7 - 10 pyrrole rings and has no correlation to dopants.

The low angle peaks in the range of 15.7 - 17.3° corresponds to the distance between two hard segments in PPy backbone which are separated by the counterion molecule. The d-spacing was reported to be affected by the alkyl chain length of the dopants (Wernet *et al.*, 1984). In this work, it is biggest for PPy/D (5.7 Å) and smallest for PPy/De, PPy/U, and PPy/P (5.1 – 5.2 Å). However, the intensity of this peak is lowest for PPy/D (9.2 %) and highest for PPy/De (14.6 %).

1.1.2 Chemical Properties

1.1.2.1 Functional Groups

The FT-IR spectra of all PPys show nearly the same features (Figure 3.3). The spectra at the wavenumber higher than 2000 cm^{-1} are featureless due to the presence of an electronic peak at ca. 1 eV or at ca. 8066 cm^{-1} (Street *et al.*, 1985). The peak at 1542-1550 cm^{-1} indicates the C=C stretching vibration (Truong *et al.*, 1997) while the peak locating between 1033-1045 cm^{-1} identifies the N-H bending of pyrrole unit (Tian and Zerbi, 1990). There are noticeable differences in PPy metrics due to the presence of the dopant anions. For example, the peak at 1700 cm^{-1} of PPy/AB indicates the stretching vibration of C=O in carboxylic group (Silverstein, 1991) of the dopant anion, *p*-aminobenzoate. The small peaks at 2919-2923, 2847-2852 cm^{-1} (not shown in Figure 3.3) in PPy/D and PPy/C belong to the asymmetric and symmetric CH_2 stretching (Silverstein, 1991) of the long aliphatic chain in the dodecylbenzene sulfonate dopant and of the camphor sulfonate dopant. They are partially covered by the electronic peak. The peak between 1170-1178 cm^{-1}, belonging to asymmetric stretching vibration of SO_2 in non-aromatic sulfonate (Pouchert, 1997), is present in the spectra of PPy/E and PPy/C. The peak locating around 615-618 cm^{-1} is the characteristic peak of the sulfonate group (ν S-O) (Prissanaroon *et al.*, 2000). It appears in all doped PPy spectra, including the PPys doped with the non-sulfur-containing dopants and the undoped PPy. This indicates the presence of co-dopant, HSO_4^- and SO_4^{2-} from the oxidant used (Ayad, 1994; Prissanaroon *et al.*, 2000). The absence of this peak in PPy/De shows the success of the dedoping process.

1.1.2.2 Nitrogen Compositions

Figure 3.4 shows the X-ray photoelectron spectrum of PPy/A in the region of N 1s. The main N peak of PPy/A centering at 399.4 eV can be attributed to the neutral N of the pyrrole ring, –NH- (Pfluger *et al.*, 1983; Pfluger and Street, 1984; Erlandsson *et al.*, 1985; Eaves *et al.*, 1987). The small shoulder at the lower binding energy side can be defined as a structural defect in the form of imine-

like nitrogen, =N- (Skotheim *et al.*, 1984). Compared to the position of the main –NH- peak, the shoulder at about 1.5 eV and about 3.1 eV higher binding energy can

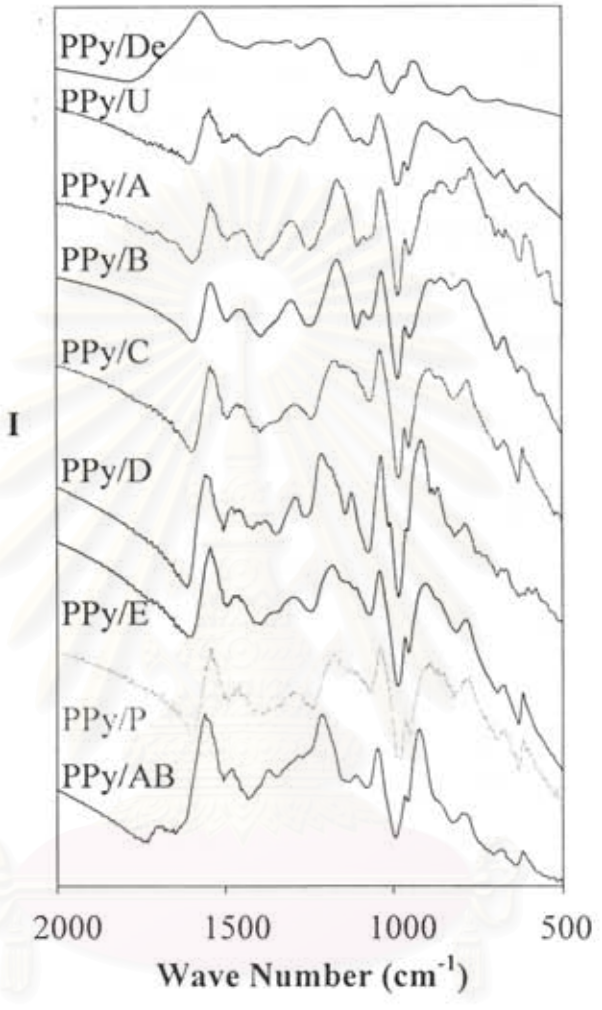

Figure 3.3 The FT-IR spectra of PPys.

สถาบันวิทยบริการ
จุฬาลงกรณ์มหาวิทยาลัย

be attributed to $-NH^{\cdot+}-$ in the polaron charge carrier species (Malitesta *et al.*, 1995), and to $=NH^{+}-$ which is a bipolaron charge carrier species (Malitesta *et al.*, 1995), respectively. The compositions of these species are shown in Table 2.

The proportion of imine-like nitrogen defect (=N-) is highest for PPy/De. This was caused by the dedoping process which was carried out in water and air. The proportions of polaron and bipolaron species and the effect of these three species on the specific conductivity are discussed below.

1.1.2.3 Charge Carrier Species

The charge carrier species in PPys as characterized by UV-Vis spectroscopy, MSB, and XPS are shown in Table 2.

The visible spectra were obtained only from the PPys that are soluble in *m*-cresol, i.e. PPy/A, PPy/B and PPy/D: their spectra are shown in Figure 3.5. The $\pi-\pi^*$ transition and the mid-band gap transition of the polaron state correspond to the maximum absorption at about 420 and 650 nm, respectively (Shen and Wan, 1997). The $\pi-\pi^*$ transition and the mid-band gap transition of the bipolaron state give the maximum absorption at about 380 and 800 nm, respectively (Shen and Wan, 1997). The visible spectra of PPy/A and PPy/B films clearly show that there are both polaron and bipolaron states as the charge carrier species. Bipolaron state is very dominant in PPy/A film whereas its proportion is small in PPy/B film. In the visible spectrum of PPy/D film, only bipolaron state was observed.

ศูนย์วิทยทรัพยากร
จุฬาลงกรณ์มหาวิทยาลัย

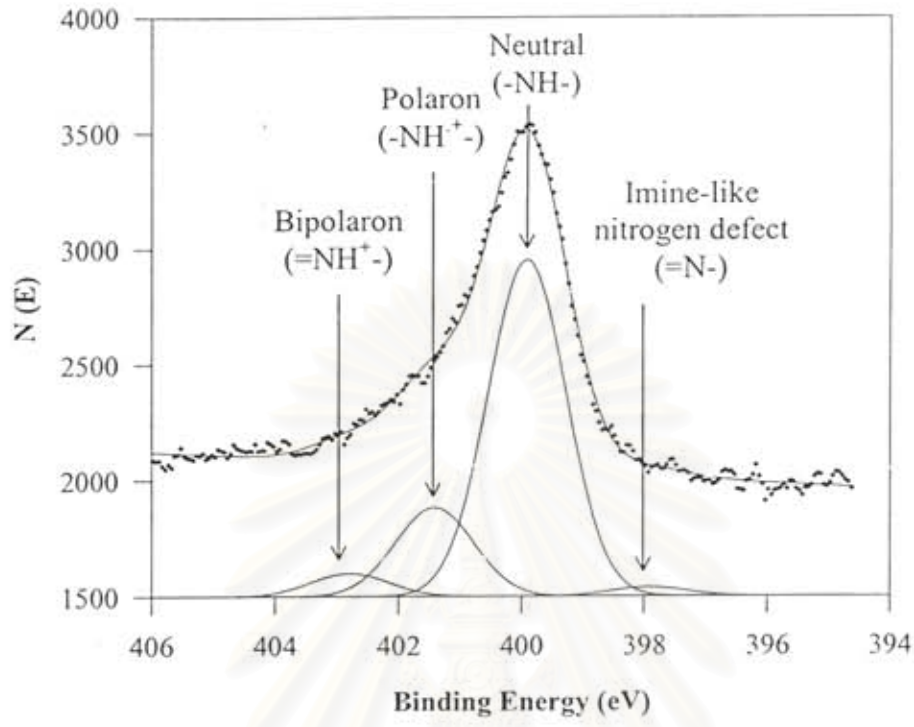

Figure 3.4 The X-ray photoelectron spectrum of PPy/A in the region of N 1s.

สถาบันวิทยบริการ
จุฬาลงกรณ์มหาวิทยาลัย

Table 2 The charge carrier species as characterized by UV-Vis, MSB, and XPS techniques (with their proportions) and the doping levels as characterized from EA, SEM/EDS, XPS, in terms of atomic ratio and charge ratio, and the specific conductivity at the age of ca. 2 months and of more than 1 year of the dedoped PPy, the undoped PPy, and the doped PPys with various dopants when fed D/M ratio was 1/12

Material	Proportion of =N+ defect	Charge Carrier Species			Doping Level				□□ (A) (S/cm)	□□ (B) (S/cm)	(B-A)/A x 100 (%)
		From UV-Vis	From MSB	From XPS	from EA (atomic ratio)	from SEM/EDS (atomic ratio)	from XPS (atomic ratio)	from XPS (charge ratio)			
PPy/De	21.6 *(16.2)*	N/A	Bipolaron or none	Polaron	N/A	0.01 *(0.01)*	0.05	0.12	7.0E-06 *(1.2E-06)*	N/A	N/A
PPy/U	2.8 *(1.0)*	N/A	Bipolaron or none	Polaron	0.12 *(0.01)*	0.11 *(0.01)*	0.12	0.26 *(0.04)*	3.9E+00 *(1.4E+00)*	5.9E-02 *(2.4E-02)*	-9.8E+01
PPy/A	2.2 *(1.4)*	Polaron &Bipolaron	Polaron *(&Bipolaron)*	Polaron, 0.21 &Bipolaron, 0.06	0.24	0.23 *(0.01)*	0.26 *(0.00)*	0.27 *(0.02)*	2.6E+01 *(4.2E+00)*	1.7E+01 *(1.1E+00)*	-3.5E+01
PPy/B	1.4 *(2.1)*	Polaron &Bipolaron	Polaron *(&Bipolaron)*	Polaron, 0.27 &Bipolaron, 0.03	0.26 *(0.00)*	0.24 *(0.02)*	N/A	0.29 *(0.00)*	3.2E+01 *(3.2E+00)*	1.3E+01 *(2.8E+00)*	-5.9E+01
PPy/C	11.6 *(9.7)*	N/A	Polaron *(&Bipolaron)*	Polaron, 0.20 &Bipolaron, 0.02	N/A	0.15 *(0.04)*	N/A	0.22 *(0.02)*	3.3E+00 *(1.1E-01)*	2.6E-01	-8.0E+01
PPy/D	7.2 *(1.7)*	Bipolaron	Bipolaron or none	Polaron, 0.20 &Bipolaron, 0.02	N/A	0.24 *(0.05)*	N/A	0.22 *(0.02)*	1.1E-01 *(7.8E-03)*	9.2E-02 *(5.2E-02)*	-1.6E+01
PPy/E	2.2 *(3.2)*	N/A	Polaron *(&Bipolaron)*	Polaron, 0.21 &Bipolaron, 0.04	N/A	0.13 *(0.05)*	N/A	0.25 *(0.05)*	3.7E+00 *(2.4E-01)*	1.6E-01 *(2.6E-02)*	-9.6E+01
PPy/P	18.5 *(1.2)*	N/A	Polaron *(&Bipolaron)*	Polaron	N/A	0.15 *(0.03)*	N/A	0.20 *(0.01)*	8.4E-01 *(3.3E-02)*	2.9E-01 *(3.3E-02)*	-6.5E+01
PPy/AB	15.8 *(0.8)*	N/A	Polaron *(&Bipolaron)*	Polaron	N/A	0.24 *(0.02)*	N/A	0.14 *(0.02)*	1.7E-03 *(2.1E-04)*	3.7E-05	-9.8E+01

The negative values of $\chi_{corr,M}$ of PPy/De, PPy/U, and PPy/D (see Table 2), reveals the diamagnetic nature and the absence of the polaron species in these PPys. For PPy/D, it confirms the result from UV-Vis technique. PPy/A, PPy/B, and other doped PPys have positive $\chi_{corr,M}$ values. This suggests their paramagnetic nature and confirms the presence of the polaron species in PPy/A and PPy/B revealed by UV-Vis technique. However, the presence of bipolaron which is not detectable by MSB can not be excluded. It is denoted in Table 2 by parentheses.

The charge carrier at the surface of PPy particles can be extracted from the XPS technique which is highly sensitive to surface composition. At the surface of PPy/De, PPy/U, and PPy/D, polaron species were detected; whereas, they are absence in the bulk. For PPy/C, PPy/E, and PPy/AB, XPS techniques shows the presence of the polaron state in their bulks as revealed by MSB. The polaron proportion is highest for PPy/B. The bipolaron species were detected only in PPys doped with the sulfonate dopants: PPy/A, PPy/B, PPy/C, PPy/D, and PPy/E. The results from XPS shows that at the surfaces of PPy/P and PPy/AB, there are only polaron species.

1.1.2.4 Doping Level

The doping levels obtained from EA, SEM/EDS, and XPS are shown in Table 2. Note that EA results correspond to the bulk properties of PPys whereas the other two techniques are surface sensitive and provide the elemental compositions at the surface. XPS provides doping levels both in terms of the atomic ratio of dopant to pyrrole's nitrogen (e.g. S/N for PPy doped with one-sulfur-containing dopant) and the charge ratio (N^+/N).

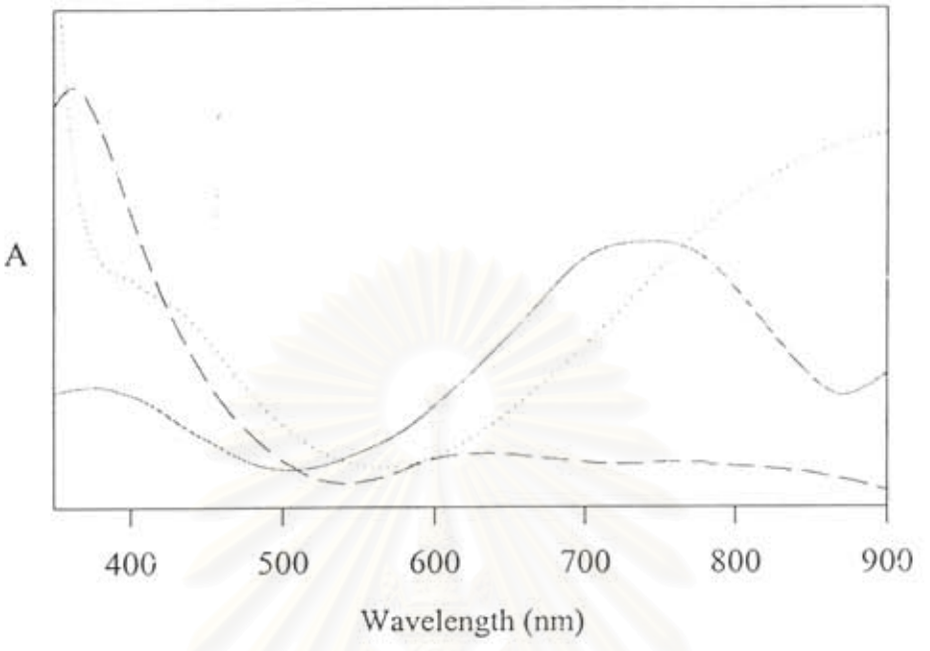

Figure 3.5 The visible spectra of soluble PPy films cast from *m*-cresol solution: (·····) PPy/A, (– – –) PPy/B, and (——) PPy/D.

สถาบันวิทยบริการ
จุฬาลงกรณ์มหาวิทยาลัย

For PPy/De, the absence of dopant is confirmed by the S/N value less than 0.05 from EDS and XPS techniques. Nevertheless, the doping level at the surface in terms of N^+/N as revealed by XPS is higher. For PPy/U, the doping level in terms of S/N from EA shows an excellent agreement with that from EDS. However, they are lower than the doping level at the surface in terms of N^+/N from XPS by a factor of two. These suggest the presence of non-sulfur containing co-dopants from environment at the surfaces of PPy/De and PPy/U. For PPy/A and PPy/B, the doping levels of bulk have a good agreement to their surfaces. Moreover, there are good agreements of S/N and N^+/N. These show the high efficiencies of α- and β-naphthalene sulfonate dopants. PPy/D also has a good correlation between S/N and N^+/N, nevertheless, the presence of polaron only at its surface could be derived from presence of HSO_4^- and SO_4^{2-} from oxidant, which provide polaron species only at the surface. In the case of PPy/AB, the atomic ratio of dopant molecule to pyrrole repeating unit is higher than the charge ratio, N^+/N. This indicates the presence of inactive molecules of *p*-aminobenzoate dopant. These molecules do not stabilize the positive charge of PPy but stick onto PPy backbone via the dispersive force attributed from benzene ring and the dipole-dipole interaction attributed from high polar -COOH group. The doping levels in terms of N^+/N of PPy/C, PPy/E, and PPy/P are higher than those expressed in terms of the atomic ratios. This indicates the presence of unknown dopant from environment. The effect of these findings on their specific conductivity values is discussed below.

1.1.3 Electrical Properties

1.1.3.1 Specific Conductivity at the Age of Two Months

Table 2 shows the specific conductivity values of PPys at the age of two months measured in the Ohmic regime of each sample. PPy/De has the specific conductivity as low as 7×10^{-6} S/cm whereas that of PPy/U is ca. six orders of magnitudes higher. Not all of doped PPys have higher specific conductivity than the undoped one. PPy/D and PPy/P have one order of magnitude lower in specific conductivity than PPy/U, whereas that of PPy/AB is as lower as three orders of magnitudes. PPy/C and PPy/E have approximately the same specific conductivity as

PPy/U. The specific conductivity is improved by nearly one order of magnitude when α- or β-naphthalene sulfonates were used as the dopants.

PPy/De has a very low specific conductivity due to the absence of dopant (see Table 2). The introduction of dopant from the environment occurred at its surface where polaron species are found (see Table 2). The presence of co-dopants in PPy/U as discussed earlier corresponds to the unexpectedly high specific conductivity and its black color. When PPy was polymerized under the presence of studied dopants, those co-dopants can be replaced. The α- and β-naphthalene sulfonate dopants can replace them effectively as proved by the very good agreement from the two terms of doping levels: N^+/N and S/N, from all techniques. For PPy/D, even its S/N and N^+/N ratios are approximately the same (see Table 2), the presence of polaron only at its surface indicates a lower of oxidation state at the particle boundaries. This could lead to the failure of electron conduction mechanism and its low conductivity. With the similar doping levels of PPy/C, PPy/E, and PPy/P, they have the specific conductivity in the same order of magnitude as PPy/U. PPy/AB has a very low specific conductivity because the inactive *p*-aminobenzoate molecules interrupt the electrical transportation in PPy as discussed above. For all PPys, the specific conductivity values clearly show the exponential correlation toward N^+/N with R^2 of 0.88.

The existence of =N- defect seems to hinder the specific conductivity of PPy as in the case of PPy/De and PPy/P. However, the exponential correlation between the proportion of =N- defect and the specific conductivity has R^2 of 0.63 only.

1.1.3.2 The Specific Conductivity at the Age of More Than One Year and the Stability in Conductivity

After storage in the ambient pressure, temperature, and humidity, the specific conductivity values of PPys were remeasured at the age of ca. one year. The stability in conductivity was calculated from the percent change in the specific conductivity from ca. two months to ca. one year, and they are shown in Table 2. Disregarding the PPy/De whose pellets were so brittle such that all them

were broken and not usable, PPy/U has the poorest conductivity stability whereas PPy/D has the best conductivity stability. PPy/A and PPy/B have moderately good stability in conductivity.

The stability in conductivity can be directly predicted from difference in doping levels in terms of S/N and N^+/N. When S/N is less than N^+/N, there are unknown dopants from environment that provide only polaron at the surface, leading to the discontinuity of oxidation state at the surface of PPy and finally conductivity decay. This was the case of most PPys, especially PPy/U. On the other hand, when doping levels in terms of S/N and N^+/N are close to each other, PPys tend to have a good stability in conductivity. The examples of this case are PPy/A, PPy/B, and PPy/D.

1.2 Effect of Dopant to Monomer Molar Ratios on Properties of PPy

Since there is no significant change in many properties of PPy/A at various dopant to monomer molar ratios (D/M ratios), only some changes in properties are discussed here.

1.2.1 Physical Property: Moisture Content

When the D/M ratio is increased from 0/1 (PPy/U) to 1/1, the moisture contents are slightly decreased from 5.6 wt % to 1.4 wt % (see Figure 3.6). Because there is no significant difference in order aggregation of PPy/A with various D/M ratios, this moisture content decrease could be explained by the increase of co-dopants which are hydrophobic (see below).

1.2.2 Chemical Property: Doping Level

For PPy/A, the doping level was determined from two expressions: N^+/N and S/N, and by two different techniques; XPS and EA. Figure 3.7a shows the doping levels of PPy/A as a function of fed D/M. Because the amount of the yielded PPy directly depends on the amount of fed oxidant, according to our unpublished data, not on the amount of fed monomer, the ratio of dopant to oxidant (D/APS ratio) is worth discussing and is included in this figure. The doping levels in terms of N^+/N

from XPS agree well with those from EA, which was determined for only some samples. As the D/M ratio increases, the doping level in terms of S/N increases and reaches the saturated value at 0.30 –0.35 when D/M ratio is 1/6 and when D/APS is very close to unity. Meanwhile, the doping level in terms of N^+/N remains steady between 0.24 – 0.27 within the whole range of fed D/M ratio. The difference in the binding energy of S IV and S VI (Descostes *et al.*, 2000) allows us to distinguish the α-naphthalene sulfonate dopant (S IV) and the HSO_4^- and SO_4^{2-} co-dopants (S VI). The results are shown in Figure 3.7b as a function of D/M ratios. In PPy/U (D/M = 0), there is no S IV: there is only S VI of co-dopants. In the presence of α-naphthalene sulfonate even at a very small amount; e.g. 1/96, it exists as dopant, replacing the co-dopants. Amounts of both dopant and co-dopants are slightly increased and levels off as the same trend as the amount of total S in Figure 3.7a. The ratio of co-dopants to dopant is varied from 1/4 to nearly unity and it seems to be uncontrollable when the D/M ratio is higher than 1/6.

The good agreement between S/N data from XPS, which is the surface sensitive technique, and S/N data from EA, which contains information of the bulk, indicates a good distribution of sulfur-containing dopants in PPy/A matrices. The excess amount of N^+/N over S/N at low D/M ratios informs the presence of non-sulfur-containing dopants. With higher D/M ratios during polymerization, α-naphthalene sulfonate dopant can replace not only co-dopants from oxidant (see Figure 3.7b), but also those unknown dopants (see Figure 3.7a). However, at D/M ratios higher than 1/12, S/N exceeds N^+/N and the ratio of co-dopants to dopant seems uncontrollable. This is due to overwhelming of the dopant molecules in the reactor during polymerization. The increase in amount of S VI of co-dopants from oxidant (Figure 3.7b) corresponds to the decrease of the moisture content as the D/M ratio increases. These co-dopants are inorganic and APS itself has very low moisture content (see Figure 3.6).

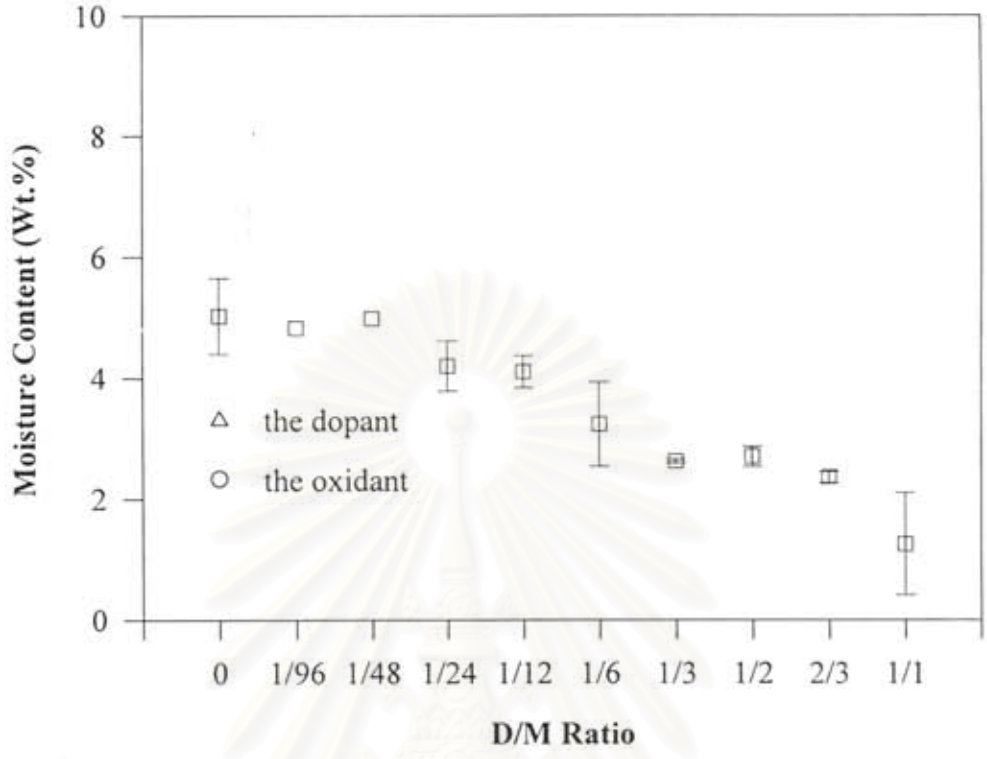

Figure 3.6 The moisture content of: (□) PPy/A at various D/M ratios; (△) α-naphthalene sulfonate (the dopant); and (○) APS (the oxidant).

สถาบันวิทยบริการ
จุฬาลงกรณ์มหาวิทยาลัย

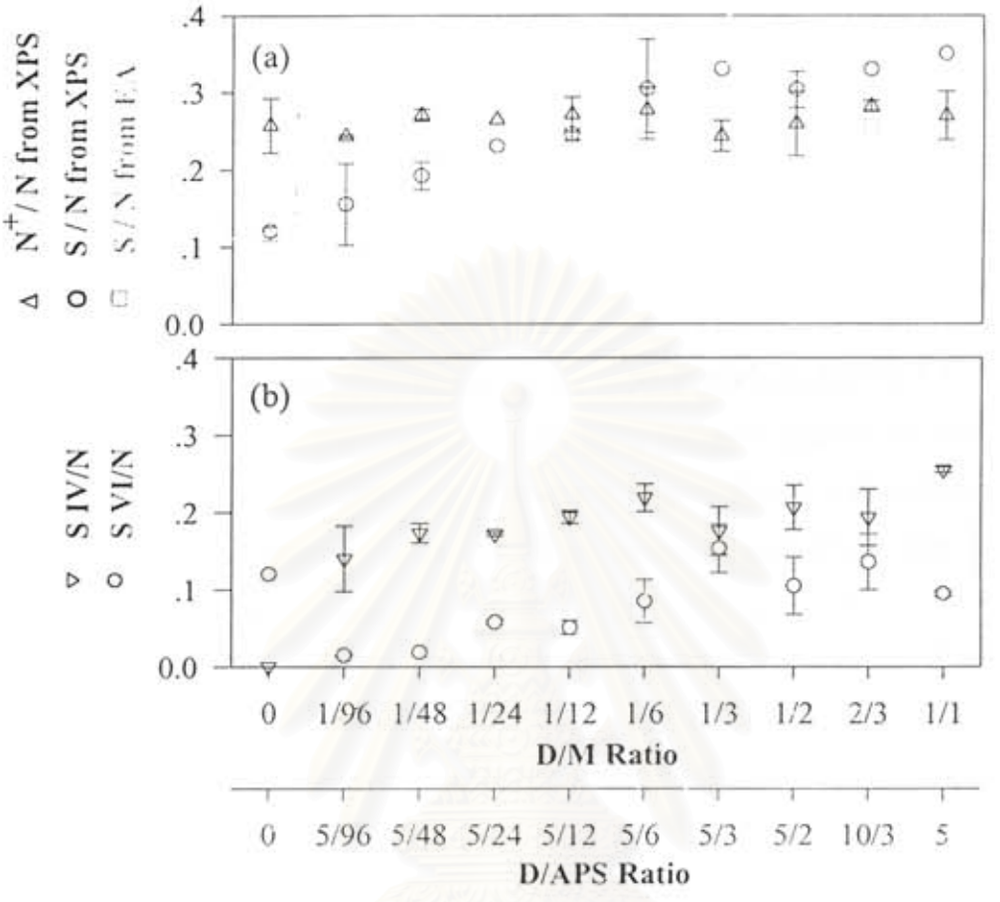

Figure 3.7 a) The doping levels in terms of: (△) N^+/N and (○) (S IV & S VI)/N from XPS; and (□) S/N from EA of PPy/A as a function of fed D/M ratios and D/APS ratios: and b) the ratios of (▽) S IV and (●) S VI toward N.

สถาบันวิทยบริการ
จุฬาลงกรณ์มหาวิทยาลัย

3.1.2.1 Electrical Properties

3.1.2.3.1 Electrical Conductivity at the Age of Two Months

As seen in Figure 3.8, the specific conductivity of PPy/A with increasing D/M ratios firstly increases from 3 (PPy/U) to 26 S/cm at D/M ratio of 1/48. It then remains constant until D/M exceeds 1/12: the specific conductivity drops down to be around 10 S/cm.

The change in the specific conductivity as the D/M ratio was varied can be explained by considering the doping levels in Figure 3.7. At the D/M ratios less than 1/48, the specific conductivity increases due to the increase of α-naphthalene sulfonate dopant which provides a better charge stabilization and higher conductivity. Beyond D/M ratio of 1/24, the specific conductivity does not increase further because the doping level is very close to the stable value, 0.25 (see Figure 3.7) (Salmon *et al.*, 1982). The decrease in the specific conductivity is evident when D/M ratio is higher than 1/12 and when S/N is slightly higher than N^+/N (see Figure 3.7). There is an excess amount of dopant which does not act as a charge stabilizer, and hinder the conductivity. The D/M ratio of 1/12 corresponds to the D/APS or dopant to yield ratio of ca. 1/3: this is consistent with that reported by the chemical analysis of PPy/ClO_4 (Street *et al.*, 1982).

3.1.2.3.2 The Specific Conductivity at the Age of More Than One Year and the Stability in Conductivity

The specific conductivity values of PPy/A at various D/M ratios measured at the age of more than one year are shown in Figure 3.8. This set of data shows the same trend but with less specific conductivity than those of PPy/A at the age of two months. As considered from the decrement of specific conductivity, when the ratio of α-naphthalene sulfonate dopant to pyrrole monomer or D/M ratio increases from 0 to 1/12, the stability in conductivity is improved. Beyond this D/M ratio, the stability is varied between 35 – 65 % based on the specific conductivity at the age of two months.

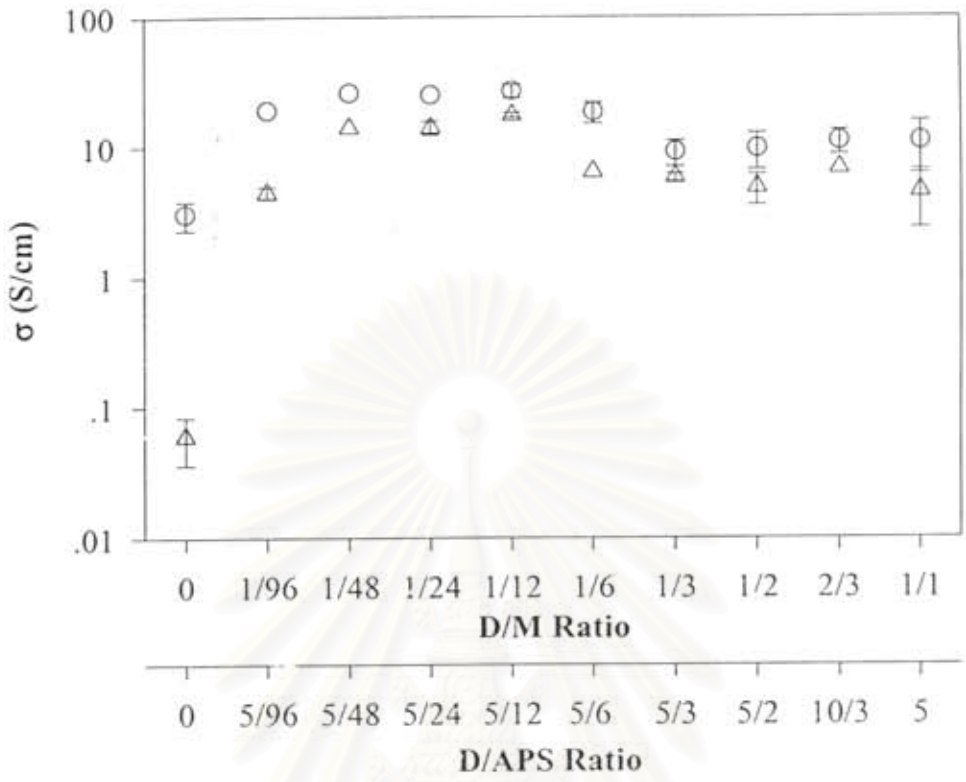

Figure 3.8 The specific conductivity of PPy/A at various D/M ratios and D/APS ratios, measured at the age of: (○) two months and (△) more than one year.

สถาบันวิทยบริการ
จุฬาลงกรณ์มหาวิทยาลัย

Part II Electrical Response of Polypyrrole to Acetone Vapor

3.2.1 Effect of Dopant Anions on the Response of PPys toward Acetone Vapor

During exposures to acetone vapor at the concentration of 17 vol.% in N_2, the specific conductivity of PPys decreased. The changes in conductivity are reversible after an evacuation overnight. The magnitudes of the equilibrium specific conductivity decrement, $-\Delta\sigma$, depend on the type of dopants existing in PPys. Figure 3.9 shows a plot of the electrical responses in terms of $-\Delta\sigma$, along with the specific conductivity of the fresh PPys, and their nitrogen compositions: imine-like nitrogen defect (=N-); polaron species ($-NH^{\cdot+}-$); and bipolaron species ($=NH^{+}-$).

A PPy with a larger amount of N^+ (polaron and bipolaron species) and correspondingly higher specific conductivity has a higher response toward acetone vapor. PPy/A and PPy/B have an outstanding sensing ability. Their $\Delta\sigma$ values are -0.2 to -0.4 S/cm, respectively. On the other hand PPy/AB, which was reported as the ineffectively doped PPy, has the poorest response: -1.5×10^{-4} S/cm. It has a low N^+ quantity, no bipolaron species, and a larger proportion of imine-like nitrogen defect, =N. PPy/U has a higher proportion of unknown dopants from the air, in addition to HSO_4^- and SO_4^{2-} from oxidant. This causes the large variation in its response toward acetone. For the sulfonate doped PPys; i.e. PPy/A, PPy/B, PPy/C, PPy/D, and PPy/E, the $-\Delta\sigma$ values at 17 vol.% acetone vapor have an exponential dependency on the doping level in terms of N^+/N and their initial specific conductivity values with the goodness of fit, R^2 of 0.80 and 0.79, respectively. Moreover, these $-\Delta\sigma$ values have almost linear dependencies on the proportion of bipolaron species and the order aggregation, which is the proportion of the overall area of X- ray diffractogram excluding the broad maxima at 2θ of 25.4 – 27.8°, with R^2 of 0.63 and 0.65, respectively.

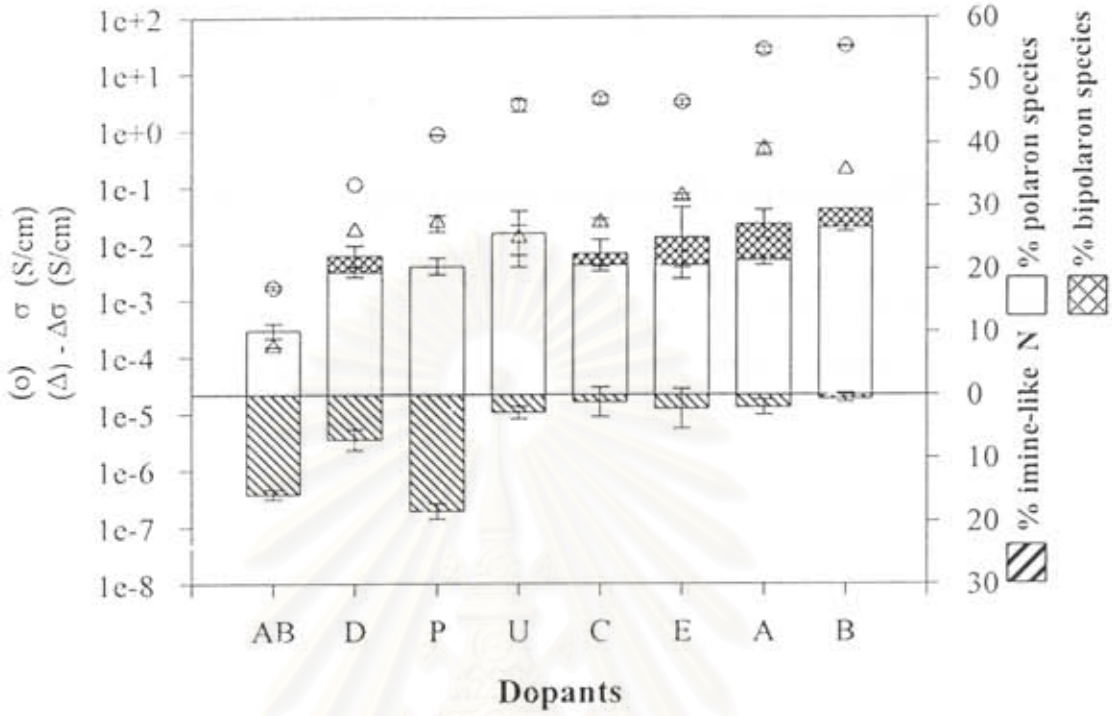

Figure 3.9 The electrical responses of PPys to acetone vapor at the concentration of 17 vol.% in N_2 in terms of $-\Delta\sigma$, at 25 ± 1 °C and at 50 ± 10 %RH, plotted with the specific conductivity of the fresh PPys and their nitrogen compositions: imine-like nitrogen (=N-); polaron (-NH^+-); and bipolaron (=NH^+-) species.

สถาบันวิทยบริการ
จุฬาลงกรณ์มหาวิทยาลัย

In summary, PPy/A and PPy/B are found to be the most promising materials for sensing acetone and PPy/AB has the lowest response toward acetone vapor. They were selected for the next experiment along with PPy/U.

3.2.2 Effect of Acetone Vapor Concentrations on the Response of PPys

Figure 3.10 shows $-\Delta\sigma$ of PPy/U, PPy/A, PPy/B, and PPy/AB when exposed to different acetone vapor concentrations. Due to the small responses of PPy/U and PPy/AB, their signals shown in this Figure 3.were multiplied by factors of 10 and 100, respectively. Some parameters, the response pattern and the sensitivity in the region of LEL to UEL of acetone and the maximum detectable concentration, are tabulated in Table 3.3.

PPy/U, PPy/A, and PPy/B have approximately linear electrical responses toward acetone vapor in the range of its LEL – UEL. PPy/AB has a non-linear one; it has a logarithmic response. The sensitivity, which is the slope of the plot, of these four PPys are in the order of PPy/A > PPy/B > PPy/U >> PPy/AB. Beyond the UEL of acetone, the first three PPys still have the linear responses until they reach their maximum detectable concentrations which are as high as ~25 vol.%. The maximum detectable concentration of PPy/AB is only 3 vol.%, this value can be clearly observed in the logarithm plot.

สถาบันวิทยบริการ
จุฬาลงกรณ์มหาวิทยาลัย

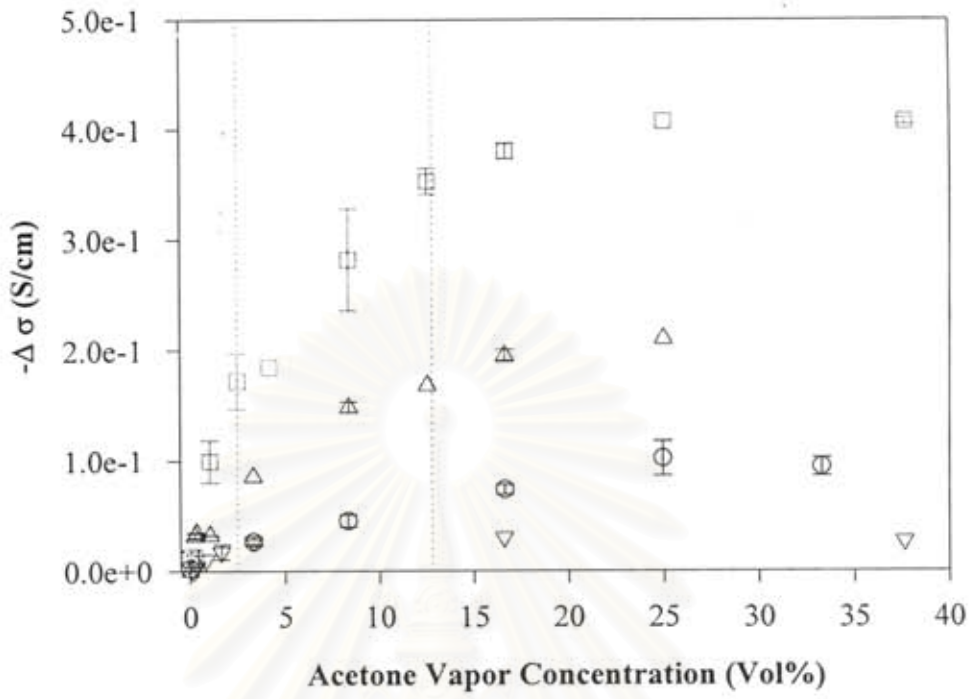

Figure 3.10 The electrical responses of: (□) PPy/A; (△) PPy/B; (○) PPy/U (x 10); and (▽) PPy/AB (x 100) to acetone vapor at various concentrations in N_2 at 25 ± 1 °C and at 50 ± 10 %RH.

สถาบันวิทยบริการ
จุฬาลงกรณ์มหาวิทยาลัย

Table 3.3 The type of response, the sensitivity, and the maximum detectable concentration of some PPys toward acetone vapor in N_2

Material	Type of response	Sensitivity in the range of LEL-UEL			Maximum detectable concentration (vol.% of acetone vapor)
		Slope (S/cm)/(vol.% of acetone vapor)	Intercept (S/cm)	R^2 of linear fits	
PPy/U	Linear	-3.0E-04	-1.7E-03	0.90	~25 %
PPy/A	Linear	-1.8E-02	-1.2E-01	0.93	~25 %
PPy/B	Linear	-9.1E-03	-6.3E-02	0.91	~25 %
PPy/AB	Non-linear	-2.0E-06	-3.0E-04	0.25	~3 %

สถาบันวิทยบริการ
จุฬาลงกรณ์มหาวิทยาลัย

The linear responses of PPy/A, PPy/B, and PPy/U imply that they can be used as linear sensors for acetone. The highest sensitivity toward acetone vapor of PPy/A correlates with the high proportion of bipolaron species present. The lowest sensitivity toward acetone vapor of PPy/AB correlates with its high proportion of imine-like nitrogen. The high acetone vapor susceptibility of PPy/A, PPy/B, and PPy/U conforms to their high concentrations of charge carrier species (both polaron and bipolaron). On the other hand, PPy/AB has the lowest maximum detectable concentration: it has the lowest amount of charge carrier species. Moreover, the concentration of the imine-like nitrogen defect in PPy/AB is very high. This defect hinders both conductivity and response toward acetone vapor. Due to the highest sensitivity of PPy/A, α-naphthalene sulfonate dopant was selected for the next experiment.

3.2.3 Effect of Dopant Concentrations on the Response of PPy/A toward Acetone Vapor

Figure 3.11 shows a plot of the electrical responses in terms of $-\Delta\sigma$, along with the specific conductivity of the fresh PPy/U and PPy/A at various D/M ratios, and their nitrogen compositions: imine-like nitrogen defect (=N-); polaron species (-NH^{+}-); and bipolaron species (=NH^{+}-). Under the presence of 17 vol.% of acetone vapor, $-\Delta\sigma$ of PPy/A becomes larger as D/M ratio increases up to 1/24. The response then levels off at $-\Delta\sigma$ equals to 0.34 S/cm (± 0.06 S/cm) beyond this D/M ratio.

As shown previously, with a larger amount of D/M ratio, PPy has a smaller amount of moisture content. The decrease in moisture content conforms to the enhancement of the response toward acetone. Moreover, the compromise between the proportion of bipolaron species and that of =N- defect is crucial. The optimum D/M ratios for acetone detection are 1/24 – 1/6 when there are large amount of bipolaron species and small amount of =N-. Beyond these ratios, due to the being overwhelmed of dopant molecules during polymerization, the proportions of these species are unpredictable. This leads to larger uncertainty in the responses.

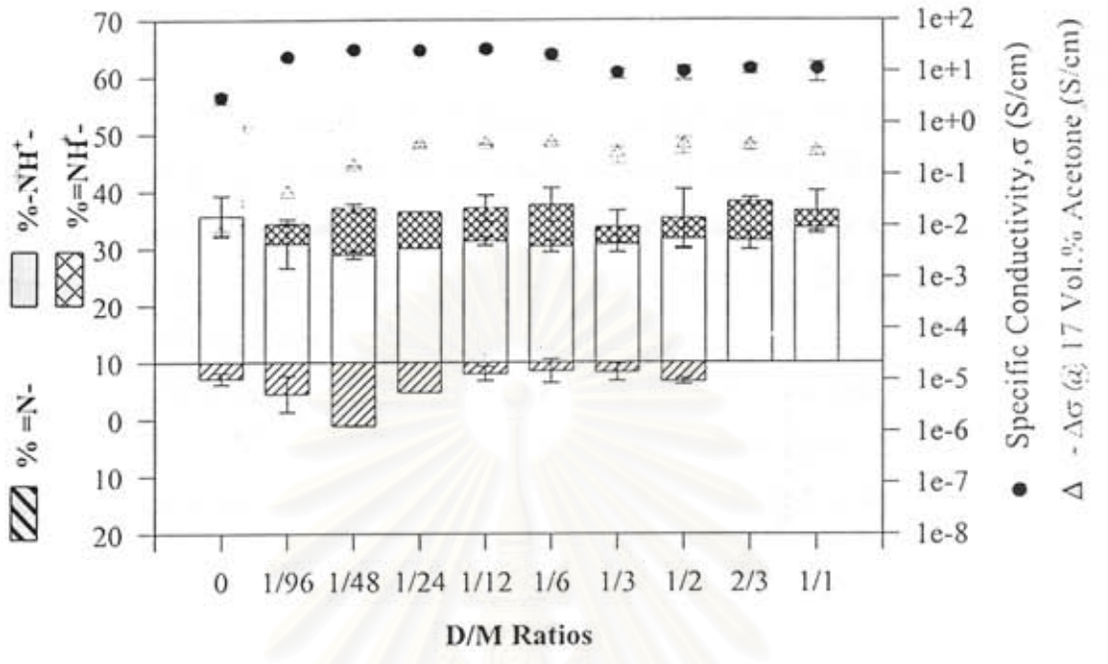

Figure 3.11 The electrical responses of PPy/A at various D/M ratios to acetone vapor at the concentration of 17 vol.% in N_2 in terms of $-\Delta\sigma$, at 25 ± 1 °C and at 50 ± 10 %RH, plotted with the specific conductivity of the fresh pellets and their nitrogen compositions: imine-like nitrogen (=N-); polaron ($-NH^{+}-$); and bipolaron ($=NH^{+}-$) species.

สถาบันวิทยบริการ
จุฬาลงกรณ์มหาวิทยาลัย

3.2.4 Investigation of Interaction between Acetone Vapor and PPy

Figure 3.12 shows the ESEM pictures of pellet surface of PPy/B before and after exposure to the saturated acetone vapor in N_2 for 24 hours. At the magnification of 46x, the overall surface of the pellet increased in irregularity upon the acetone exposure. At the magnification of 3500x, it was evident that the globular structure got some swelling after a prolonged acetone exposure.

The XPS results reveal no significant change in the chemical species of PPy upon a prolonged exposure to acetone vapor (figure is not shown). This is due to a very high vacuum system and the nature of XPS for being a very high surface sensitive technique. This confirms the *reversibility* of interaction between acetone and PPy.

The X-ray diffraction patterns of the PPy/A before and after immersing in acetone liquid for 30 minutes are shown in Figure 3.13 along with their deconvoluted results underneath. The most significant change after the exposure is the decrease in the proportion of the peak at 2θ of 17.0° (SD = 0.7°; d-spacing = 5.4 Å) which corresponds to the distance between two hard segments in PPy backbone which are separated by the counterion molecules (Wernet *et al.*, 1984). This change is accompanied by the increase of the peak at 2θ of 20.6° (SD = 0.2°; d-spacing = 4.3 Å) which can be identified as the distance between neighboring pyrrole rings on the same chain (Davidson *et al.*, 1996 and Gassner *et al.*, 1997) when α-α' linkages are single bonds. The second most significant change in X-ray diffractograms can be clearly seen only from the deconvoluted results. It is the proportions of two diffraction peaks at the 2θ around 25.5° (d-spacing = 3.5 Å). These two peaks can be defined as an interplanar spacing between aromatic pyrrole units from two different chains or segments (Allen *et al.*, 1997). The sharper peak indicates the presence of the extent of crystalline domains as large as 32 Å, whereas the broader one corresponds to the disorder proportion in PPy. The area ratio of the sharper peak to the broader one is 1.3 (SD = 0.1) for the fresh PPy/A. It decreases to be 0.6 (SD = 0.1) after immersing in acetone liquid for 30 min. This change indicates that acetone destroys the dispersion force between aromatic pyrrole units and increases the

disorder section in PPy which hinders the electron mobility and hence decreases the specific conductivity of PPy. This result agrees with the conclusions given above that a PPy with a higher proportion of order aggregation has a higher response to acetone.

The TGA thermogram of the PPy/B after an exposure to the saturated acetone vapor for 24 h (Figure 3.14) shows a desorption of chemicals when the temperature was increased to 180 - 240 °C. This temperature is well above the boiling point of acetone (56.1 °C). The result suggests the chemisorption of acetone in the PPy matrix during the prolonged exposure.

The FT-IR spectrum of the PPy/D after exposure to the saturated acetone vapor for 24 h (Figure 3.15) confirms the above statement. The stretching vibration of C=O group in acetone adsorbed onto PPy (Figure 3.15b) has a frequency of 1709-1713 cm^{-1}: lower than that of C=O group in acetone vapor: 1738 cm^{-1} (Figure 3.15c). This was probably caused by the hydrogen-bonding formation between C=O group of acetone and N-H group of pyrrole repeating unit. This hydrogen-bonding weakened the C=O bond by forming a new O···H bond using the lonepair electrons of O in carbonyl group. This finding answers the inverse correlation between acetone response and the presence of =N- which is a non-donator for H-bonding. Moreover, it was found that, from the experimental study to determine the effect of dopant to monomer molar ratio of PPy/A on the response toward acetone vapor, as the ratio increases, the moisture content is lower due to the presence of hydrophopic dopant and the electrical response toward acetone vapor is enhanced. This is because the existing water molecules decrease the amount of active sites for acetone (neutral and charged -NH-) and increase the amount of =N- in PPy, as evidenced by XPS (Erlandsson *et al.*, 1985).

Upon exposure to the saturated acetone vapor, the absorbances of peaks in visible spectrum of PPy/B film evidently decreased, as shown in Figure 3.16. The peak reduction agrees with the change observed by Blackwood and Josowicz (1991) upon an exposure to methanol vapor of the PPy/TCNQ film. This was claimed to result from the reduction in polaron and bipolaron species in the film because methanol acts as a reducing agent toward PPy. The same reason is also applicable for this acetone exposure. Acetone as a reducing agent conforms to the finding that

acetone reduces the conductivity of PPy. The decreases in bipolaron were found to be more dominant than those of polaron (-89%, SD = 9% and –33%, SD = 9%, respectively). This may explain the best sensitivity of PPy/A which possesses the highest proportion of bipolaron. Note that there was no significant change in the transition energies observed.

สถาบันวิทยบริการ
จุฬาลงกรณ์มหาวิทยาลัย

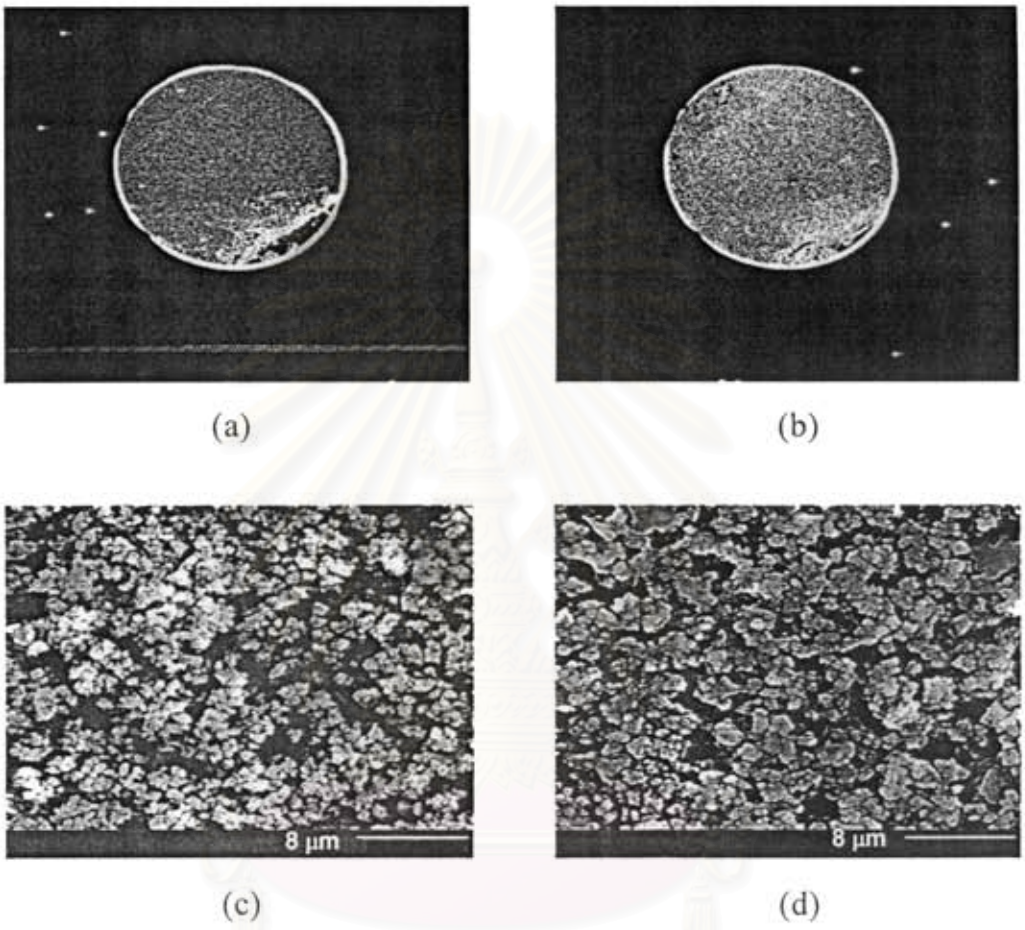

Figure 3.12 The morphology of PPy/B pellet: a) before and b) after exposure to the saturated acetone vapor in N_2 for 24 hours at the magnification of 40x: c) before and d) after exposure to the saturated acetone vapor for 24 hours at the magnification of 3500x.

สถาบันวิทยบริการ
จุฬาลงกรณ์มหาวิทยาลัย

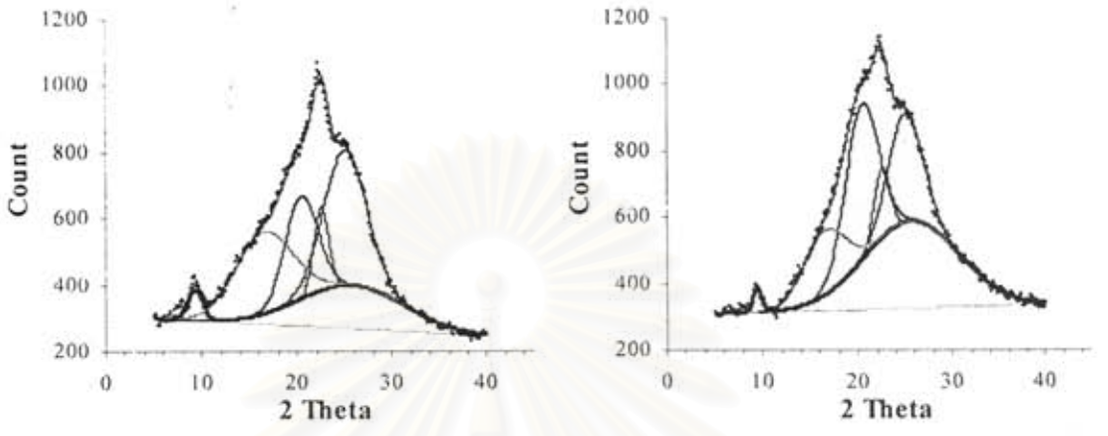

Figure 3.13 The X-ray diffractograms of: a) fresh PPy/A pellet; and b) the same PPy/A pellet after immersing in the acetone liquid for 30 min, with their deconvoluted results underneath.

สถาบันวิทยบริการ
จุฬาลงกรณ์มหาวิทยาลัย

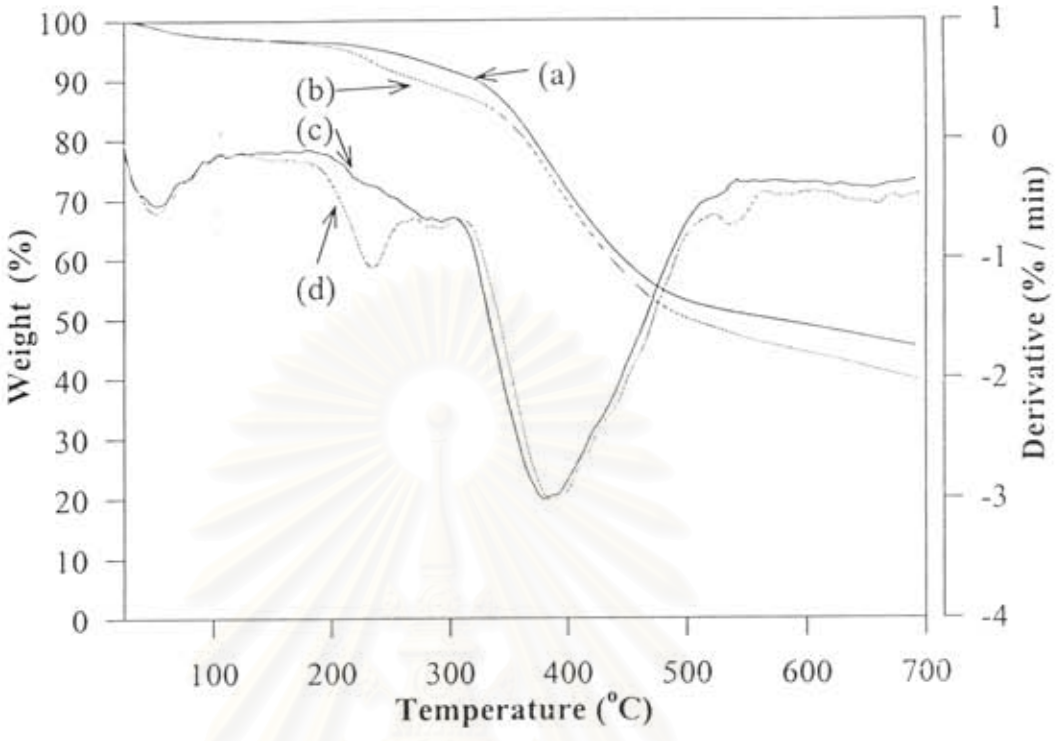

Figure 3.14 The TGA thermograms of: a) fresh PPy/B; and PPy/B after the exposure to the saturated acetone vapor in N_2 for 24 hours; and their derivatives c) and d), respectively.

สถาบันวิทยบริการ
จุฬาลงกรณ์มหาวิทยาลัย

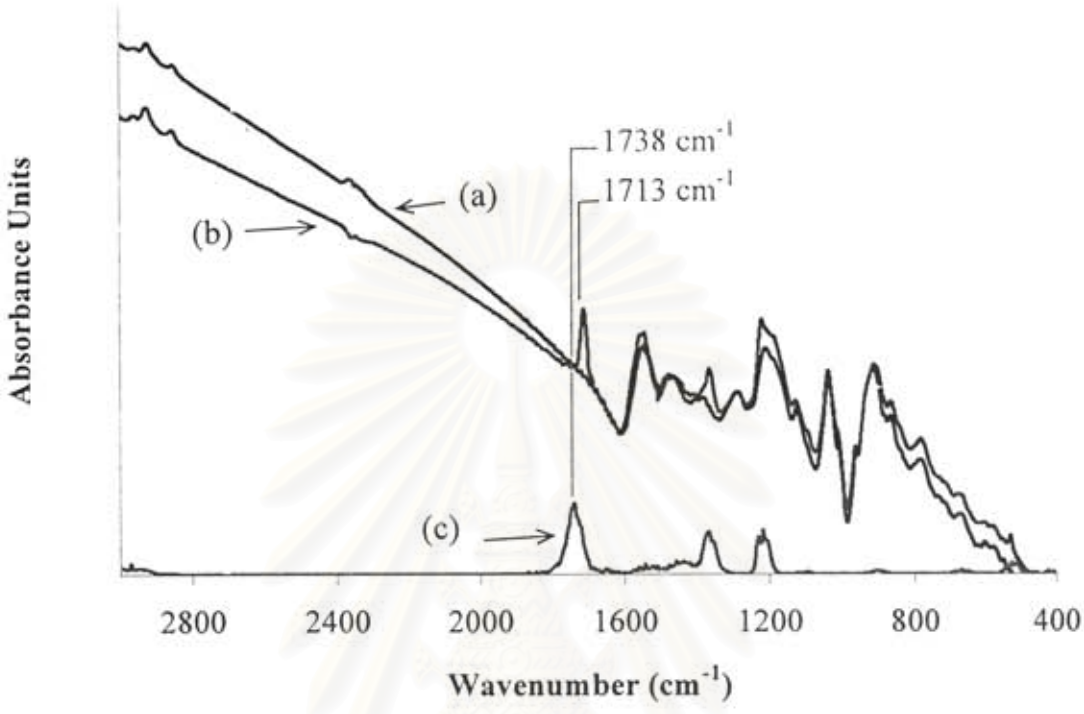

Figure 3.15 The FT-IR spectra of: a) fresh PPy/D; b) PPy/D after the exposure to the saturated acetone vapor in N_2 for 24 hours; and c) acetone vapor.

สถาบันวิทยบริการ
จุฬาลงกรณ์มหาวิทยาลัย

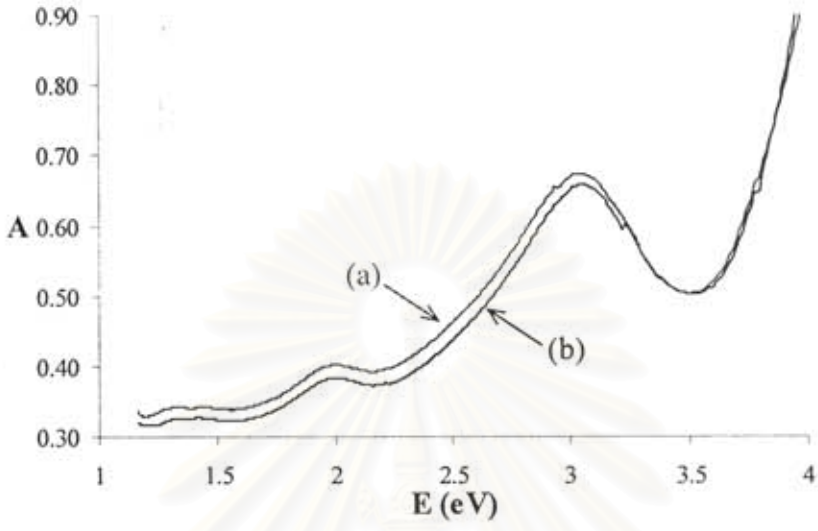

Figure 3.16 The visible spectra of: a) the fresh PPy/B film, and b) the same film upon exposure to saturated acetone vapor.

สถาบันวิทยบริการ
จุฬาลงกรณ์มหาวิทยาลัย

CHAPTER IV
CONCLUSIONS AND RECOMMENDATIONS

4.1 Conclusions

Among seven dopants used in this work, α-naphthalene sulfonate and β-naphthalene sulfonate are the most suitable ones for PPy by an *in-situ* doped polymerization process. They provide PPy with the best mechanical, chemical and electrical properties. As increasing amount of α-naphthalene sulfonate dopant during polymerization, the α-naphthalene sulfonate-doped PPy (PPy/A) has better electrical properties. The maximum doping level in terms of N^+/N is 0.24 - 0.27. The dopant to monomer molar ratio (D/M ratio) giving PPy/A with the highest specific conductivity and stability is 1/12. This D/M ratio corresponds to the ratio between the dopant and the yielded PPy of about 1/3, which is close to the maximum N^+/N obtained. Beyond the D/M ratio of 1/12, the dopant molecules become overcrowded during polymerization. This hinders the electron conduction mechanism.

The electrical sensitivity to acetone vapor of conductive PPys was modified by utilizing various types of dopant and various dopant concentrations during polymerization. The dopants which provide PPy with higher specific conductivity, higher order aggregation, higher proportions of charge carrier species, especially bipolaron ($-NH^{\cdot+}-$), and lower proportion of imine-like nitrogen defect (=N-) are the effective ones in improving the sensitivity to the acetone vapor. The PPy/A and the β-naphthalene sulfonate-doped PPy (PPy/B) are the most promising candidates amongst PPys investigated as polymeric sensor materials used in detecting acetone vapor. The optimum D/M ratios for this application are 1/24 – 1/6.

As investigated by ESEM and XRD, acetone penetrated and swelled PPy. Its molecules diffused into the intersegmental spaces in the PPy matrices, which were previously separated by the dopant molecules. They also destroyed the dispersing forces between aromatic pyrrole rings, as evidenced by XRD. Acetone molecules chemically absorbed onto a PPy matrix *via* a hydrogen-bonding, as seen by TGA and FT-IR. These interactions hindered the electron jumping and hence decreased the

specific conductivity of PPy. Moreover, the presence of water molecules in the form of moisture content in PPy matrix seemed to suppress the response to acetone by reducing the accessible active sites (neutral and charged –NH-). The changes in visible spectra of PPy/B during an acetone exposure indicated the reduction of charge carrier species, especially bipolaron. This explains the best sensitivity of PPy/A and PPy/B which have relatively high proportion of charge carries species, especially bipolaron in PPy/A.

4.2 Recommendations for Future Work

The gas sensing experiment in this work has been carried out in N_2 atmosphere. The preliminary result when using synthetic air as a carrier gas, composing of O_2 and N_2, in stead of N_2, was done but not reported here. Even though our results show no difference between these two carrier gases, the effect of O_2 in synthetic air on the sensing performance of PPy-based gas sensor is interesting for further investigation, especially, for a prolonged exposure and at a high temperature. Under the presence of O_2, interactions between PPy and chemical vapors are expected to be more complicated, especially at high temperature. However, if the results can be understood, a possibility of having an inexpensive and portable online-sensor for these flammables chemical seems likely.

สถาบันวิทยบริการ
จุฬาลงกรณ์มหาวิทยาลัย

REFFERENCES

Allen, N.S., Murray, K.S., Fleming, R.J., Saunders, B.R. (1997) Synth. Met. 87, 237.

Angeli, A. (1916) Gazz. Chim. Ital., 46 279.

Ayad, M.M. (1994) J. Appl. Polym. Sci., 53, 1331.

Blackwood, D., Josowicz, M. (1991) J. Phys. Chem. 95, 493.

Blanc, J.P. (1990) Sensor and Actuators, B41, 130.

Briggs, D. (1998) Surface Analysis of Polymers by XPS and Static SIMS, 1st ed., Cambridge: Cambridge University Press, p 49-51.

Buncick, M.C., Thomas, D.E., McKinny, K.S., Jahan, M.S. (2000) App. Surf. Sci., 156, 97.

Campbell, D., White, J.R. (1991) Polymer Characterization, 2nd ed. Great Britain at the University Press, Cambridge, p. 163.

Cao, Y., Smith, P., Heeger, A.J. (1992) Synthetic Metals, 48, 91.

Cassignol, C., Olivier, P., Ricard, A. (1998) Journal of Applied Polymer Science, 70, 1567.

Chiu, H.-T., Lin, S.-J., Huang, C.-M. (1992) J. Appl. Electrochem., 22, 358.

Chou J. (2000) Hazardous gas monitors. 1st ed., New York: McGraw-Hill book company.

Dall'Olio, A., Dascola Y., G.P., Gardini, G.P. (1969) C.R. Acad. Sci., 267, 4336.

Davidson, R.G., Hammond, L.C., Turner, T.G., Wilson, A.R. (1996) Synth. Met. 81, 1.

Deng, Z., Stone, D. C., Thompson, M. (1997) Analyst, 122, 1129.

Descostes, M., Mercier, F., Thromat, N., Beaucaire, C., Gautier-Soyer, M. (2000) Appl. Surf. Sci. 165, 288.

Eaves, J.G., Munro, H.S., Parker, D. (1987) Polym. Commum. 28, 39.

Erlandsson, R., Inganas, O., Lundstrom, I., Salaneck, W.R. (1985) Synth. Met. 10, 303.

Gassner, F., Graf, S., Merz, A. (1997) Synth. Met. 87, 75.

Grulke, E. A. (1989) Solubility parameter values. In J. Brandrup, E.H. Immergut (Eds.), Polymer handbook. 3rd ed., (pp. VII/519 – 559).

Gustafsson, G., Lundstrom, I. (1987) Synthetic Metals, 21, 203.

Hanawa, T., Yoneyama, H. (1989) Bulletin Chemical Society of Japan, 62, 1710.

Harris, D. P., Arnold, M.W., Andrews, K.M., Partridge, C.A. (1997) Sensor and Actuators, B: Chemical, B42, 177.

Heeger, A.J., MacDiarmid, A.G. (1980) in The Physics and Chemistry of Low Dimensional Solids, L. Alcacer (ed), D. Reidel Pub. Co., Boston, pp. 353-391.

Hodgins, D. (1995) Sensors and Actuators, B26-27, 255.

http://www.crowcon.com

Hwang, B.J., Yang, J.Y, Lin C.W. (1999) J. Electrochem. Soc., 146, 1231.

Josowiez, M., Janata, J., Ashley, K., Pons, S. (1987) Analytical Chemistry, 59, 253.

Kanazawa, K.K., Diaz, A.F. (1979) Synthetic Metals, 1, 326.

Kuwabata, S., Yoneyama, H., Tamura, H. (1984) Bull. Chem. Soc. Jpn. 57, 2247.

Langmaier, J., Janata, J. (1991) Polymeric Material Science and Engineering, 64, 285.

Lin C.W., Yang, J.Y., Hwang, B.J., Chin, J. (1999) Inst. Chem. Engrs., 30, 449.

Lindsey, S.E., Street, G.B. (1984) Synthetic Metals, 10, 67.

Loughlin, C. (1993) Sensor for industrial inspection. 1st ed., West Yorkshire, U.K.: Ilkley.

Malitesta, C., Losito, I., Sabbatini, L., Zambonin, P. G. (1995) J. of Electron Spectroscopy and Related Phenomena 76, 629.

Miasik, J., Hooper, A., Tofield, B. (1986) Journal of Chemistry Society, Faraday Trans., 82, 1117.

Milella, E., Musio, F., Alba, B.M. (1996). Thin Solid Films, 908.

Musio, F., Ferrara, C.M., (1997) Sensor and Actuators, B41, 97.

Okuzaki, H., Kondo, T., Kunugi, T. (1997) Polymer, 38, 5491.

Okuzaki, H., Kondo, T., Kunugi, T. (1999) Polymer, 40, 995.

Omastova, M., Kosina, S., Pionteck, J., Andreas, J., Pavlinec, J. (1996) Synthetic Metals, 81, 49.

Partridge, A.C., Harris, P., Andrews, M.K. (1996) Analyst, 121, 1349.

Pfluger, P. Krounbi, M., Street, G.B., Weiser, G. (1983) J. Chem. Phys. 78, 3212.

Pfluger, P., Street, G.B. (1984) J. Chem. Phys. 80, 544.

Philip, N.B., Sim, K.L. (1989) Sensors and Actuators, 19, 125.

Pijolat, C., Pupier, C., Sauvan, M., Tournier, G., Lalauze, R. (1999) Sensors and Actuators, B 59, 195.

Pouchert, C. J. (1997) The Aldrich library of FT-IR spectra. 2nd ed., Milwaukee, Wisconsin: Aldrich.

Prissanaroon, W., Ruangchuay, L., Sirivat, A., and Schwank, J. (2000) Electrical conductivity response of dodecylbenzene sulfonic acid-doped polypyrrole films to SO_2-N_2 mixtures. Synthetic Metals, 114(1), 65-72.

Qian, R. (1993) in Conjugated Polymers and Related Materials, W.R. Salaneck, I. Lundstrom, B. Ranby (Eds), Oxford University Press, London, p. 161.

Rodríquez, J., Grande, H.-J., Otero, T.F.(1997) Polypyrroles: from Basic Research to Technological Applications in H.S. Nalwa (Ed) Organic Conductive Molecules and Polymers. Vol. 2, 1st ed. John Wiley & Sons, England, p. 415.

Salaneck, W.R., Lundstrom, I., Ranby, B. (1993) Conjugated polymers and related materials. 1st ed., New York: Oxford Unversity Press.

Salmon, M., Diaz, A.F., Logan, A.J., Krounbi, M., Bargon, J. (1982) Mol. Cryst. Liq. Cryst. 83, 265.

Selampinar, F., Toppare, L., Akbulut, U., Yalcin, T., Suzer, S. (1995) Synthetic Metals, 68, 109.

Shen, Y.Q., Wan, M.X. (1997) Journal of Polymer Science Part A-Polymer Chemistry, 35, 3689.

Shen, Y.Q., Wan, M.X. (1998) Synthetic Metals, 96, 127.

Shirakawa, H., Zhang, Y.-X., Okuda, T., Sakamaki, K., and Akagi, K. (1994) Synthetic Metals, 65, 93.

Silverstein, R.M. (1991) Spectrometric indentification of organic compounds, John Wiley & Sons, New York, p. 117.

Skotheim, T.A., Florit, M.I., Melo, A., O'Grady, W.E. (1984) Phys. Rev. B 30, 4846.

Street, G.B., Clarke, T.C., Krounbi, M., Kanazawa, K., Lee, V., Pfluger, P., Scott, J. C., Weiser, B. (1982) Mol. Cryst. Liq. Cryst. 83, 253.

Street, G.B., Lindsey, S.E., Nazzal, A.I., Wynne, K.J. (1985) Mol. Cryst. Liq. Cryst. 118, 137.

Sun Y., Ruckenstein, E. (1996) Synthetic Metals, 82, 35.

Tian, B., Zerbi, G. (1990) J. Chem. Phys. 94, 3886.

จุฬาลงกรณ์มหาวิทยาลัย

ทุนวิจัย

กองทุนรัชดาภิเษกสมโภช

รายงานวิจัย

การเตรียมและทดสอบคุณภาพของฟิล์มพอลิพิโรล เพื่อใช้ในการตรวจวัดไอระเหยของสารเคมี

สถาบันวิทยบริการ
จุฬาลงกรณ์มหาวิทยาลัย

โดย

อนุวัฒน์ ศิริวัฒน์

ลดาวัลย์ เรืองช่วย

กันยายน ๒๕๔๕

Topart, P., Josowicz, M. (1992) Journal of Physical Chemistry, 96, 7824.

Truong, V.T., Ennis, B.C., Forsyth, M. (1995) Polymer, 36(10), 1933.

Truong, V.T., Ennis, B.C., Terrence, T.G., Jenden, C.M. (1992), 27, 187.

Truong, V.T., Terrence, B.C., Turner T.G., Jenden, C.M. (1997) Polym. Internal., 27, 187.

Wang, Z. H., Jawadi, H.H.S., Ray, A., MacDiarmid, A.G., Epstein, A.J. (1990) Phys. Rev., B 42, 5411.

Wernet, W., Mondenbusch, M., Wegner, G. (1984) Makromol. Chem., Rapid Commum. 5, 157.

Yamaura, M., Hagiwara, T., Iwata, K. (1988) Synthetic Metals, 26, 209.

Zotti, G. (1997) Electrochemical synthesis of polyheterocycles and their applications. In H.S. Nalwa (Ed) Organic conductive molecules and polymers. Vol. 2, 1st ed. (p. 415) England: John Wiley & Sons.

สถาบันวิทยบริการ
จุฬาลงกรณ์มหาวิทยาลัย